SYNTHESES OF NEW MONOMERIC AND POLYMERIC UNITS AND THEIR ELECTROCHEMICAL BEHAVIORS FOR THE USE IN ELECTROCHROMIC APPLICATIONS

A THESIS SUBMITTED TO
THE GRADUATE SCHOOL OF NATURAL AND APPLIED SCIENCES
OF
MIDDLE EAST TECHNICAL UNIVERSITY

BY

NAZLI BUKET ZAĞFOĞLU

IN PARTIAL FULFILLMENT OF THE REQUIREMENTS
FOR
THE DEGREE OF MASTER OF SCIENCE
IN
CHEMISTRY

JULY 2013

Approval of the thesis:

SYNTHESES OF NEW MONOMERIC AND POLYMERIC UNITS AND THEIR ELECTROCHEMICAL BEHAVIORS FOR THE USE IN ELECTROCHROMIC APPLICATIONS

submitted by **NAZLI BUKET ZAİFOĞLU** in partial fulfillment of the requirements for the degree of **Master of Science in Chemistry Department, Middle East Technical University** by,

Prof. Dr. Canan Özgen
Dean, Graduate School of **Natural and Applied Sciences** _____

Prof. Dr. Güner Özkan
Head of Department, **Chemistry** _____

Prof. Dr. Levent Toppare
Supervisor, **Chemistry Dept., METU** _____

Assoc. Prof. Dr. Ali Çırpan
Co-Supervisor, **Chemistry Dept., METU** _____

Examining Committee Members:

Prof. Dr. Teoman Tinçer _____
Chemistry Dept., METU

Prof. Dr. Levent Toppare _____
Chemistry Dept., METU

Prof. Dr. Mustafa Güllü _____
Chemistry Dept., AU

Assoc. Prof. Dr. Ali Çırpan _____
Chemistry Dept., METU

Assist. Prof. Dr. Özlem Erel _____
Chemistry Dept., METU

Date:

I hereby declare that all information in this document has been obtained and presented in accordance with academic rules and ethical conduct. I also declare that, as required by these rules and conduct, I have fully cited and referenced all material and results that are not original to this work.

Name, Last Name: NAZLI BUKET ZAĞFOĞLU

Signature:

ABSTRACT

SYNTHESES OF NEW MONOMERIC AND POLYMERIC UNITS AND ELECTROCHEMICAL BEHAVIORS FOR THE USE IN ELECTROCHROMIC APPLICATIONS

Zaifoğlu, N. Buket
M. S., Department of Chemistry
Supervisor: Prof. Dr. Levent Toppare
Co-Supervisor: Assoc. Prof. Dr. Ali Çırpan

July 2013, 45 pages

4'-(Tert-butyl)-4,7-di(thiophen-2-yl)spiro[benzo[d]imidazole-2,1'-cyclohexane], 4,7-di([2,2'-bithiophen]-5-yl)-4'-(tert-butyl)spiro[benzo[d]imidazole-2,1'-cyclohexane], 4'-(tert-butyl)-4,7-bis(thieno[3,2-b]thiophen-2-yl)spiro[benzo[d]imidazole-2,1'-cyclohexane] were synthesized, electrochemically polymerized and electrochromic properties of resultant polymers were investigated. The monomers were characterized by nuclear magnetic resonance spectroscopy (^{1}H-NMR, ^{13}C-NMR). Cyclic voltammetry (CV) and ultraviolet–visible spectroscopy techniques were used to investigate electrochemical behavior of the monomers and redox behaviors of the conducting polymers. After electrochemical polymerization, the electrochromic properties of the conducting polymers were investigated via spectroelectrochemical, and kinetic studies.

Poly-(2-(4-(hexadecyloxy)phenyl)-5-methyl-10-(5-methylthiophen-2-yl)-1-phenyl-1H-phenanthro[9,10-d]imidazole), poly-(2-(4-(hexadecyloxy)phenyl)-5-methyl-10-(5'-methyl-[2,2'-bithiophen]-5-yl)-1-phenyl-1H-phenanthro[9,10-d]imidazole) were synthesized and their electrochromic properties were investigated. For the characterization of the polymers gel permeation chromatography (GPC), differential scanning calorimetry (DSC), and thermogravimetric analysis (TGA) were used. Cyclic voltammetry (CV) and ultraviolet–visible spectroscopy were used to investigate electrochemical behavior and redox reactions of conducting polymers.

Keywords: Donor-Acceptor-Donor, Conducting Polymers, Benzimidazole, Phenanthrene.

ÖZ

ELEKTROKROMİK UYGULAMALARDA KULLANIM AMACIYLA YENİ MONOMERİK VE POLİMERİK ÜNİTELERİN SENTEZİ VE ELEKTROKİMYASAL ÖZELLİKLERİNİN İNCELENMESİ

Zaifoğlu, N. Buket
Yüksek Lisans, Kimya Bölümü
Tez Yöneticisi: Prof. Dr. Levent Toppare
Ortak Tez Yöneticisi: Doç. Dr. Ali Çırpan

Temmuz 2013, 45 sayfa

4'-(Tert-butil)-4,7-di(tiyofen-2-il)spiro[benzo[d]imidazol-2,1'-siklohekzan], 4,7-di([2,2'-bitiyofen]-5-il)-4'-(tert-butil)spiro[benzo[d]imidazol-2,1'-siklohekzan], 4'-(tert-butil)-4,7-bis(tiyano[3,2-b]tiyofen-2-il)spiro[benzo[d]imidazol-2,1'-siklohekzan] kimyasal olarak sentezlendi, elektrokimyasal olarak polimerleştirildi ve oluşan polimerlerin elektrokromik özellikleri incelendi. Sentezlenen monomerlerin karakterizayonu nükleer manyetik rezonans spektroskopisiyle sağlandı (^{1}H-NMR, ^{13}C-NMR). Monomerlerin elektrokimyasal davranışlarını ve polimerlerin redoks reaksiyonlarını incelemek amacıyla döngüsel voltametri ve ultraviyole-görünür bölge spektroskopisi teknikleri kullanıldı. Elektorkimyasal olarak sentezlenen iletken polimerlerin elektrokromik özellikleri spektroelektrokimyasal ve kinetik çalışmalarla incelendi.
Poli-(2-(4-(hekzadesiloksi)fenil)-5-metil-10-(5-metiltiyofen-2-il)-1-fenil-1H-fenantro[9,10-d]imidazol), poli-(2-(4-(hekzadesiloksi)fenil)-5-metil-10-(5'-metil-[2,2'-bitiyofen]-5-il)-1-fenil-1H-fenantro[9,10-d]imidazol) sentezlendi ve elektrokromik özellikleri incelendi. Polimerlerin karakterizasyonu için jel geçirgenlik kromotografisi, diferansiyel taramalı kromatografi, ve termogravimetrik analiz yöntemleri kullanıldı. İleteken polimerlerin elektrokimyasal özelliklerini ve redoks reaksiyonlarını incelemek üzere döngüsel voltametri ve ultraviyole-görünür bölge spektroskopisi teknikleri kullanıldı.

Anahtar kelimeler: Donör-Akseptör-Donör, İletken Polimerler, Benzimidazol, Fenantren.

To My Parents,

ACKNOWLEDGEMENTS

I would like to express my deepest appreciation to my mentor Prof. Dr. Levent Toppare who supports me with every decision I made. Without his guidance, support and encourage I would not be the person who I am right now. His believe in my success will always help me to achieve the greatest goals. I am grateful to him beyond words for now and the future.

I appreciate the help and support of my co-advisor Assoc. Prof. Dr. Ali Çırpan. His valuable discussions taught me a lot.

I would like to thank Naime Akbaşoğlu Ünlü for the design and synthesis of the organic molecules and for her endless friendship as well.

I would like to thank all Toppare Research Group members for their help and friendship.

I would like to thank my high school chemistry teacher Güler Nayır Aydın for her support and believe in me.

Finally, I would like to thank my family and friends for their endless support.

TABLE OF CONTENTS

LIST OF FIGURES

FIGURES

CHAPTER 1

INTRODUCTION

1. 1. Conducting Polymers

The history of polymers has begun with the groundbreaking work of Staudinger in 1920 which was published with the striking title "Über Polimerisation". [1] Although polymers like rubber had been used since 1600s the existence of macromolecules was unknown until 1900s. [2] After the discovery of Staudinger the progress in polymer science has increased tremendously. In 1935 Nylon was invented by Wallace Carothers from DuPont Company. [3] Thirty years later Kevlar, the toughest polymer ever, was invented by Stephanie Kwolek. [4]

Beginning from the discovery of the macromolecules they were known to be electrically insulators. However, in 1970s this idea was changed. At the beginning of 1970s Alan Heeger was curious about chain-like metallic materials. Being a physicists he discussed his idea with a chemist MacDiarmid. Meanwhile in Japan one of Shirakawa's students was synthesized polyacetylene (PA) as a bright silvery film while it was expected to be black powder via adding 1000 fold catalyst by mistake. Mutual interest of those three scientists resulted in the discovery of electrically conductive polymer which was honored by the Nobel Prize in Chemistry in 2000. [5]

Polyacetylene is the first polymer discovered as electrically conductive by above mentioned three scientists. Albeit it has high conductivity PA has some drawbacks such as being unstable in air and insoluble in common solvents which prevents it from being commercialized. Consequently, researchers have started to seek new conjugated polymers with better characteristics in order to be used in the larger scale production. Examples of some commonly used polymers are given in Figure 1.1.

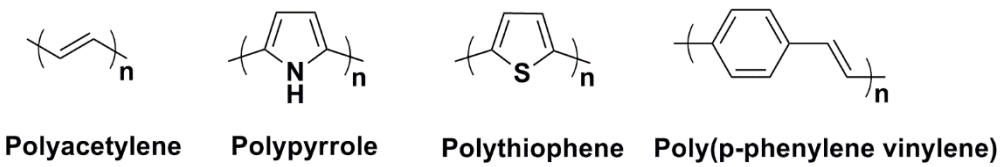

Figure 1. 1. Structures of common conducting polymers.

1. 2. Band Theory

Quantum-mechanical Bohr postulates state that the energy of an electron in an isolated atom can only have discrete values. [6] Nevertheless, when there exists a system containing a number of chemically bonded atoms, electronic orbitals do combine and form molecular orbitals. [7] As the number of chemically bonded atoms increases the number of orbitals increases as well. As a result, the energy difference between orbitals of

bonded atoms decreases and finally forms a continuous set which is called as an energy band gap. [8,9]

Materials are classified as conductors, semiconductors, and insulators according to the magnitude of their band gap. Insulators have the largest band gap, and conductors do not have a defined band gap since the valence and conduction bands are overlapped. Band gap of semiconductors lies in between the band gap of insulators and conductors. The schematic representation of band structures are given in Figure 1. 2. [10]

The Fermi level is a hypothetical energy level of an electron. At thermodynamic equilibrium this energy level have 50% probability of being occupied by the electrons. [10]

For the conduction of electricity electrons must be promoted to the conduction band with sufficient energy. In the case of conductive materials highest energy level of the valence band (HOMO) and the lowest energy level of the conduction band (LUMO) have similar energy hence the electron can easily be promoted from valence band to the conduction band. In the case of semiconductors there exists a small band gap between the valence and the conduction bands; therefore, electrons can be promoted from valence band to conduction band via thermal excitation, vibrational excitation, or excitation by photons. In the case of insulators the band gap is too large as a result promotion of electrons from valence band to conduction band cannot take place. [11]

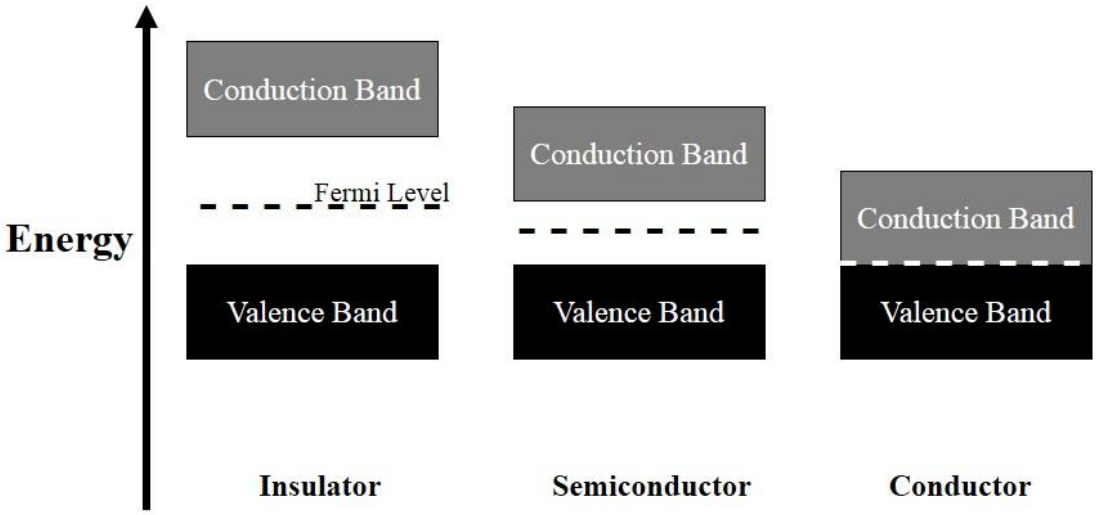

Figure 1. 2. Schematic representation of band structures**.**

In the case of conjugated polymers as the number of repeating units (mers) increases the overlap between orbitals increases forming energy bands as described above. Formation of energy bands decreases the gap between the bonding (HOMO) and anti-bonding (LUMO) orbitals which is called as band gap (Figure 1.3). Low band gap polymers are desired for electrochromic and photovoltaic applications since they are semiconductors. [12]

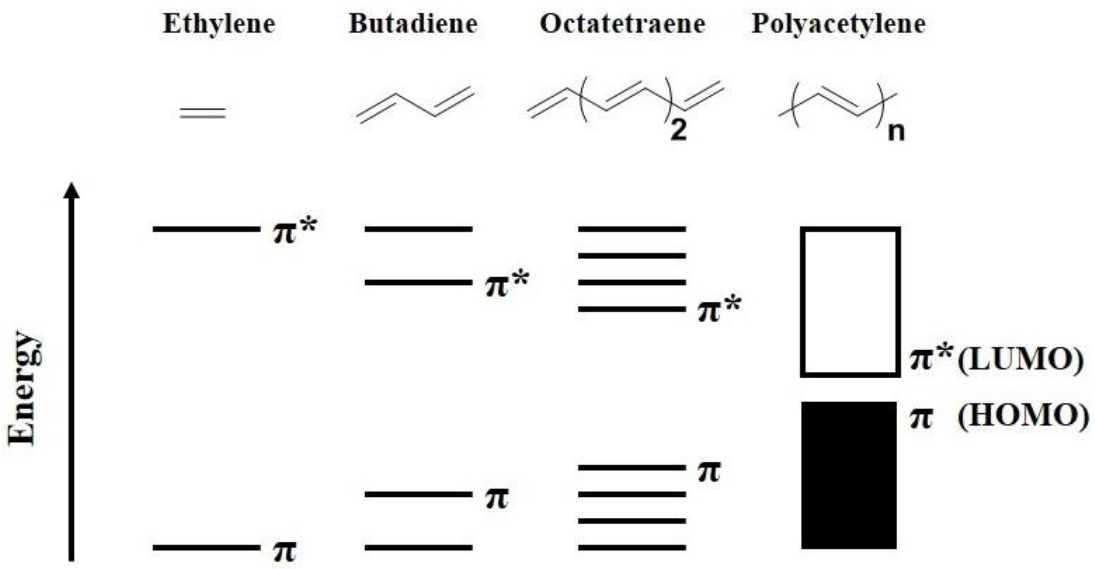

Figure 1. 3. Generation of bands in conjugated polymers.

1. 3. Conduction Mechanism of Conjugated Polymers

Doping is the incorporation of certain impurities to the polymeric system in order to enhance the conductivity of the conjugated polymer. Doping can be achieved by using protic solvents, chemically oxidizing / reducing agents, or applying a potential difference. [12] The idea behind the doping process is to partially oxidize or reduce the polymer chain. Upon oxidation (p-doping) electrons are removed from the polymer chain forming positive charges on the polymer backbone, upon reduction (n-doping) electrons are inserted into the polymers chain forming negative charges on the polymer backbone. These charges / electrons move in the polymer chain when placed in an electric field as charge / current carriers. Formation of polarons and bipolarons for polythiophene upon p-type doping is shown in Figure 1. 4.

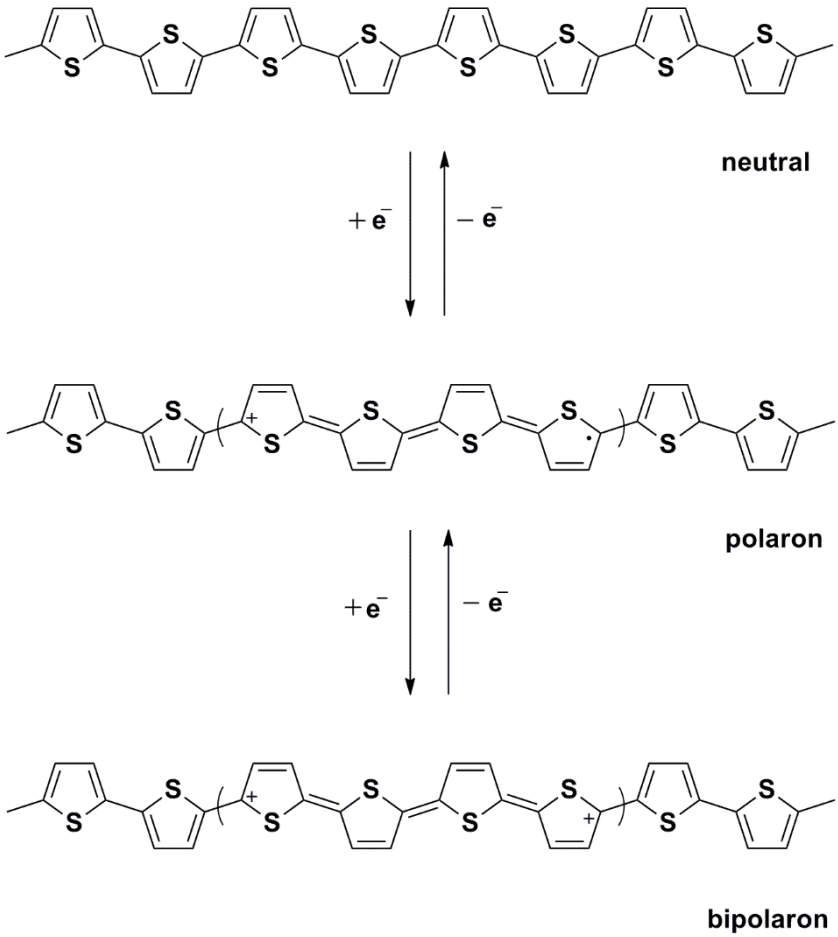

Figure 1. 4. Formation of polaron and bipolaron in polythiophene.

In the case of p-doping removal of delocalized electrons from the p-orbital of the polymer takes place. In this case Fermi level of the electrode which is in contact with the conducting polymer is below the valence band of the polymer hence electrons flow from the polymer to the electrode. Similarly, electrons are injected into the delocalized p-orbital of the polymer in the case of n-doping. The Fermi level of the electrode is above the conduction band of the polymer, therefore, electrons flow from the electrode to the polymer (Figure 1.5). [13]

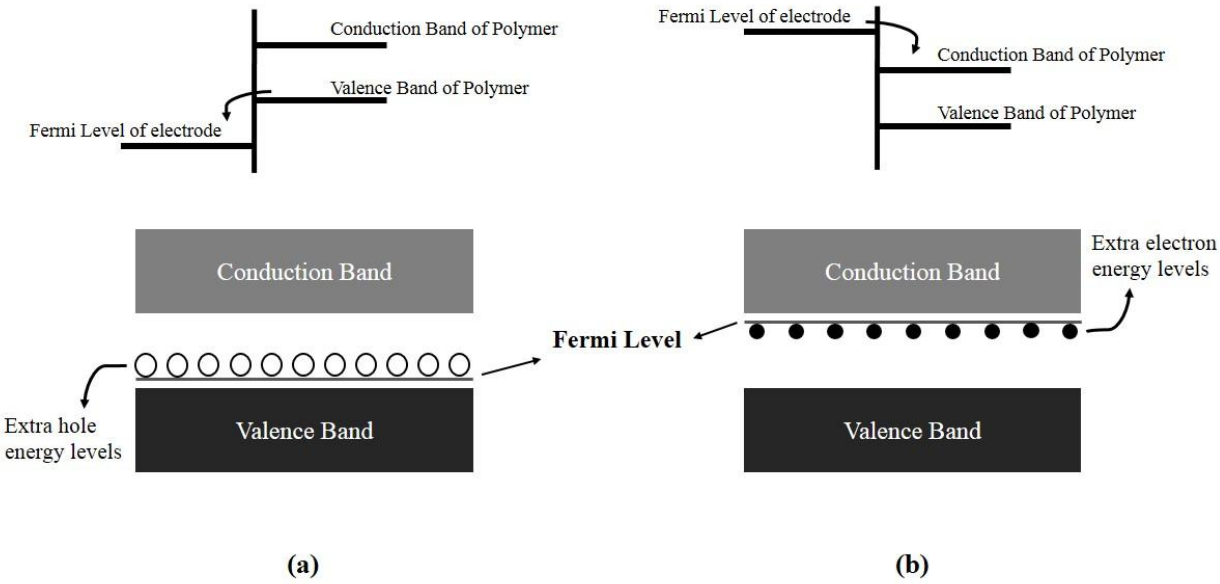

Figure 1. 5. Schematic representation of doping process for a conducting polymer; a) p-doping and b) n-doping.

1. 4. Design of Low Band Gap Polymers

Design of the polymeric structure is of high importance to obtain the low band gap polymer. There are six main factors affecting the band gap of the polymer.

i. π conjugation length
ii. Bond length alternation
iii. Planarity
iv. Aromatic resonance energy
v. Substituents
vi. Intermolecular interactions

As the conjugation length, the distance along the polymer chain with uninterrupted delocalization of molecular orbitals, increases the overlap between electronic orbitals increases which results in the decrease of the band gap. [14]

In order to decrease the difference in bond length alternation donor and acceptor units along the conjugated polymer chain is used hence the band gap is decreased. [15,16]

Increasing the planarity along the aromatic backbone decreases the band gap as a result of the higher degree of delocalization of electrons. [17]

As the aromatic resonance energy of the repeating units decreases formation of the quinoid structure becomes more favorable. Stabilization of the quinoid structure results in lowered band gap.

Electron donating substituents on the donor unit increases the electron density and electron donating ability of the donor group. In addition, electron withdrawing substituents on the acceptor group decreases the electron density and increases the electron accepting ability of the acceptor unit. [18]

1. 5. Chromism

Chromism is defined as the reversible color change of a material with the help of external stimulus. [19] There are many different types of chromism depending on the type of external stimulus. Most commonly encountered types of chromism are; thermochromism, solvatochromism, photochromism, and electrochromism.

Thermochromism is the reversible color change of a material that is triggered with heat. [20]

Solvatochromism is generally observed in metal complexes. It depends on the polarity of the solvent. [21]

Photochromism is the reversible color change of a material induced by the irradiation of the light. The idea behind the photochromism is the isomerization of the chemical structure upon electromagnetic irradiation. [22]

Electrochromism is defined as the reversible color change of a material upon applied potential. Redox couple of a material exhibits different electronic absorption bands in the visible region. The color change of a material can be between a transparent and a colored state or between two or more colored states which is called as multichromism. [23,24]

1. 6. Electrochromic Materials

According to the classification of Chang et. al. at IBM electrochromic materials can be divided into three groups as type I, type II, and type III. [25]

Type I electrochromic materials are the ones that are soluble in a given electrolyte solution both in the oxidized and the reduced state. N,N'dimethyl-4,4'-bipyridylium, metal complexes, and organic redox indicators are common examples of type I electrochromic materials.

Type II electrochromic materials are soluble in one redox state whereas insoluble in the other one. They form an insoluble solid film on the surface of an electrode. N,N'-bis(*n*-heptyl)-4,4'-bispyridylium solution in water can be an example of this type of electrochromic materials.

Type III electrochromic materials are the ones that are studied on the surface of an electrode in the form of thin films. Conducting polymers are of type III electrochromic materials.

Type II and type III electrochromic materials have optical memory meaning that once the redox state has been achieved the color of the system remains. However, for type I electrochromic materials current must flow until the whole solution is electrolyzed since the electrolyzed material diffuses away from the electrode.

1. 7. Applications of Conducting Polymers

1. 7. 1. Artificial Muscles

Artificial muscles are the materials that can reversibly change its shape either by contracting, expanding, or rotating with the help of an external stimulus. [26] Polypyrrole films are the most commonly studied ones for artificial muscle research. When an artificial muscle made of polypyrrole film is placed in electrochemical cell the flow of anodic current oxidizes the polymer by removing an electron from the chain hence changing the distribution of the double bonds and the bond angles. This conformational change results in an increase in the volume by the penetration of counter ions and water molecules to the system hence the result is swelling, a macroscopic change in the structure. Similarly, in the case of cathodic flow oxidized polymer film returns to the neutral state and the negatively charges counterions diffuse into the solution hence the polymeric system shrinks. Systematic representation for the artificial muscle is shown in Figure 1.6. [27] When perchlorate ion is used as a counter ion the chemistry of the macroscopic change can be outlined as follows;

$$(PPy)_s + (ClO_4^-)_{aq} \rightleftharpoons [(PPy)^{n+}(ClO_4^-)_n(H_2O)_m]_{gel} + ne^-$$

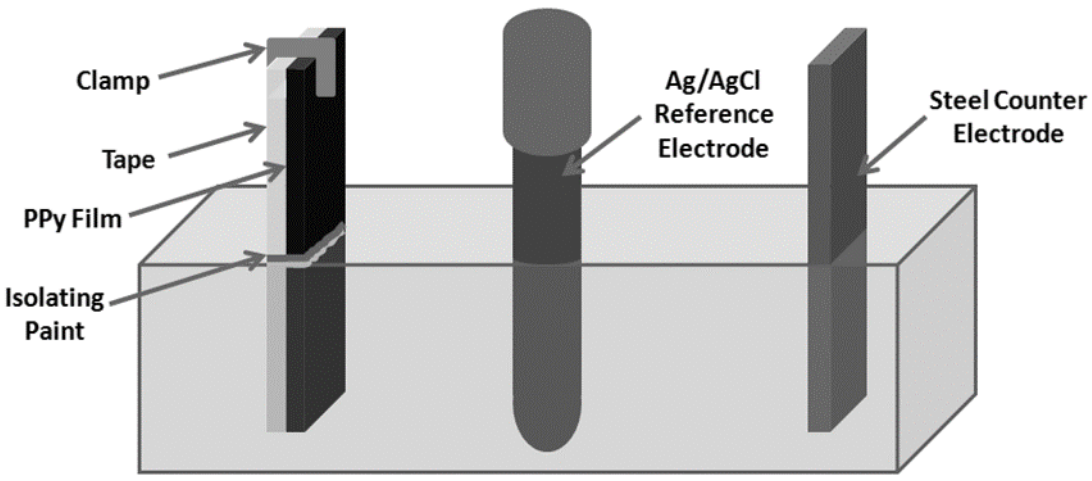

Figure 1. 6. Experimental setup of the artificial muscle.

1. 7. 2. Biosensors

Biosensor is an analytical device that is used for the detection of biological substances. In order to construct an amperometric biosensor enzyme immobilization onto the surface of an electrode is the crucial step. Immobilization of an enzyme can be achieved by different techniques such as covalent binding, physical adsorption, and entrapment in substrate. Biocompatible conducting polymers are used in the construction

of biosensors to incorporate the enzyme onto the electrode surface since they offer numerous advantages such as, strong biomolecular interactions, low detection limits, and cost effectiveness. [28]

Construction of a biosensor takes place by coating the polymer on the graphite electrode from the monomer solution via cyclic voltammetry. After the coating of the polymer onto the electrode surface, the second step is the enzyme immobilization. Construction of a biosensor is represented in Figure 1.7.

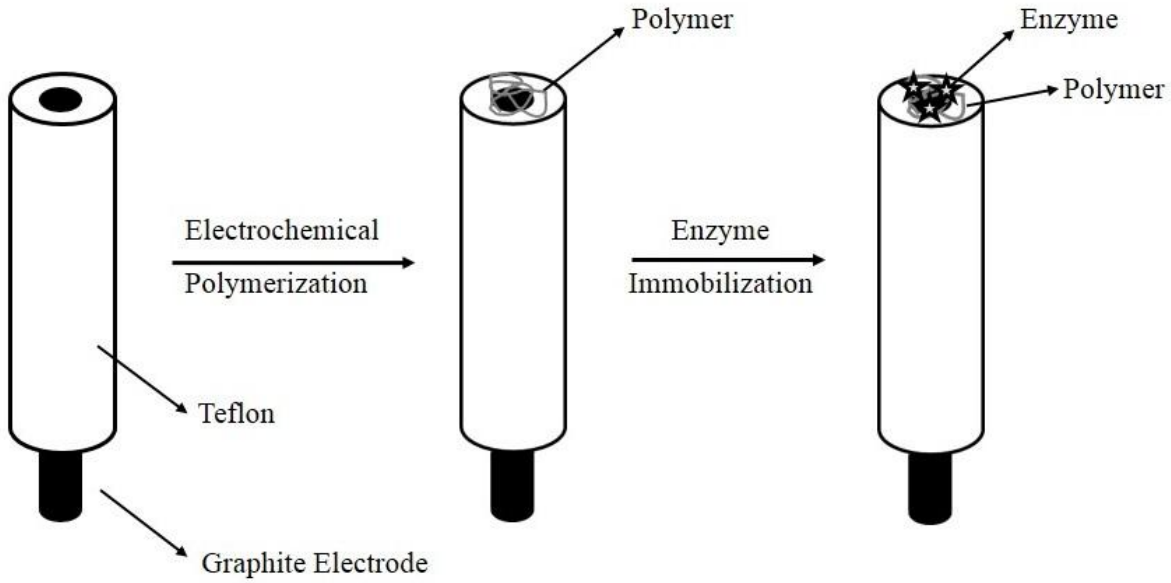

Figure 1. 7. Construction of a biosensor.

1. 7. 3. Electrochromic Devices

In recent years both in academia and industry, research based on electrochromic devices with conducting polymers has increased tremendously due to its widespread applications. Electrochromic devices are commonly used in automobile industry as car rear view mirrors, and sunroofs; architectural applications as smart windows; and military applications as camouflage materials. [29]

An electrochromic device is simply an electrochemical cell in which electrochromic electrodes are used as the redox couple. Either both of the electrodes used in the construction of an electrochromic device can be colored upon redox reaction or only one of the electrodes can be colored depending on the choice of use. Figure 1. 8 shows the representative example of an electrochromic device. [23]

When anodic potential is applied electrochromic polymer at the anode will be oxidized and the color will be changed from its neutral state color to an oxidized state one. At the same time reduction of the polymer will take place at the cathode hence the neutral state color of the polymer changes to its reduced state color. [30]

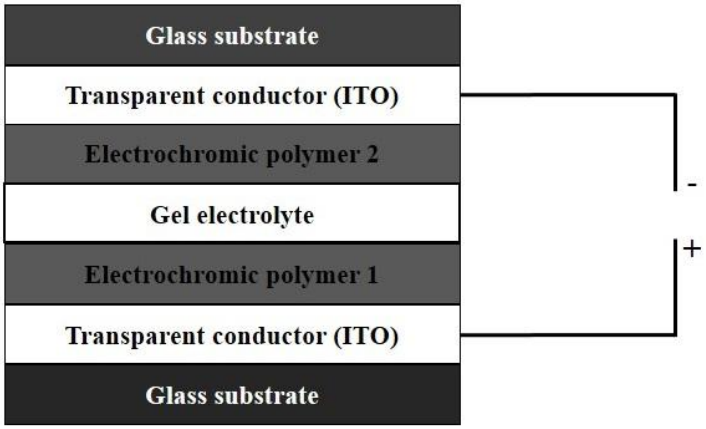

Figure 1. 8. Electrochromic device structure.

In order to produce an electrochromic device with enhanced properties such as; good stability, color uniformity, short response time, long term optical memory, high electrochromic efficiency, and high optical contrast, conducting polymers with different physical and chemical properties have been studied.

1. 7. 4. Organic Light Emitting Diodes

Organic polymers with low band gap are of crucial importance in the field of photovoltaics since a better overlap between the absorption spectrum of the polymer and the solar spectrum can improve the performance of a photovoltaic device. [31]

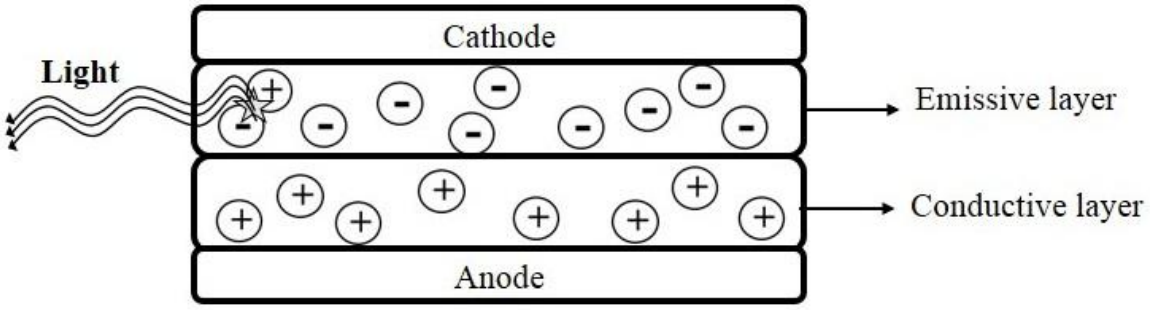

Figure 1. 9. Schematic representation of an OLED.

An organic light emitting diode (OLED) is composed of an emissive layer and a conductive layer sandwiched between the anode and the cathode. In its most simple form an OLED is constructed by coating the ITO substrate (anode) with PEDOT:PSS which functions as a hole transport layer. On PEDOT:PSS layer organic light emitting polymer is coated and then metal electrode which functions as a cathode is evaporated upon. Schematic representation of an OLED is shown in Figure 1. 9. [32]

When a potential difference is applied electrons move from cathode to the emissive layer where at the same time anode removes electrons from the conducting layer. Movement of an electron from the conductive layer to the anode can also be described as an introduction of holes from anode to the conductive layer. Therefore electrons will exist in emissive layer while holes will be in the conductive layer. Due to the electrostatic attractions between an electron and a hole they will form a bound state called as an exciton. Since the mobility of holes are higher than the mobility of electrons in organic semiconductors exciton will be formed at the emissive layer. The relaxation of an exciton takes place by an emission of radiation of a definite wavelength depending on the band gap of a material. [32]

1. 7. 5. Organic Solar Cells

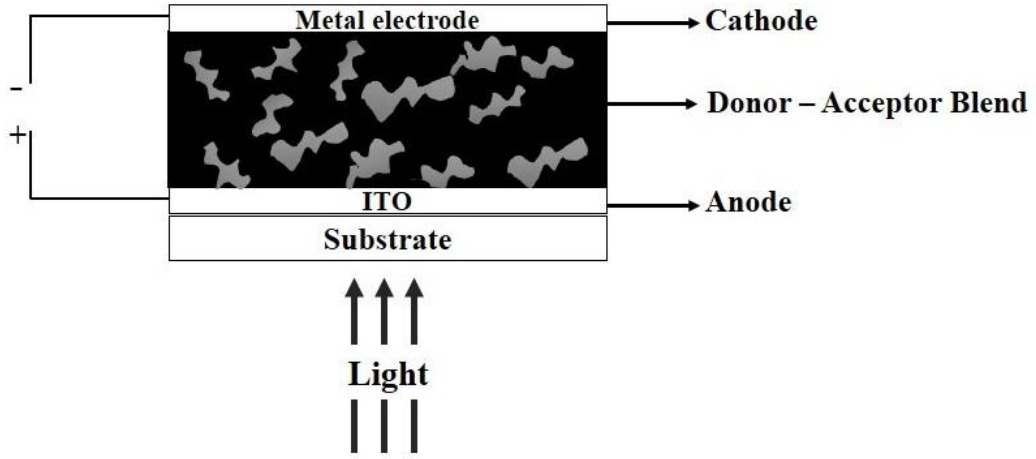

Figure 1. 10. Bulk heterojunction type organic solar cell.

A solar cell is a device which converts the energy of light into the electrical energy by means of photovoltaic effect. [33]

Solar cells based on inorganic materials like silicon have known since 1950s. [34] Later in 1970s organic solar cells were introduced. [35] Starting from 1970s research based on organic solar cells has increased tremendously since they exhibit superior properties compared to the inorganic solar cells. The most important advantage of organic solar cells is being flexible so that they can be constructed on any kind of surface. Moreover, organic solar cells are solution processable, cheap, and light-weight.

An organic cell device structure is shown in Figure 1. 10. Usually glass or PET used as a substrate with conductive layer of ITO on it. Above them there exists the active layer which is the blend of donor and acceptor moieties. Upon this active layer there exists metal electrode which functions as a cathode. [33]

The working principle of an organic solar cell starts with an absorption of sunlight. Since the substrate and ITO are transparent the sunlight goes directly into the active layer. The absorption of light with certain energy causes an excitation of an

electron from the valence band to the conduction band leaving a positively charged electron hole behind. The excited electron which is in the conduction band is attracted to the electron hole which is in the valence band by Columbic attraction. This bound state of an electron and a hole that are attracted to each other by electrostatic Coulomb force is called as an exciton. If the difference between the LUMO levels of the donor and acceptor is equal or higher than the binding energy of an exciton, the exciton tends to dissociate. The excited electron moves from the LUMO of the donor to the LUMO of the acceptor and then to the cathode. At the same time the hole moves from the HOMO of the donor to the anode. With the effective dissociation of an exciton the production of electricity is achieved (Figure 1. 11). [33]

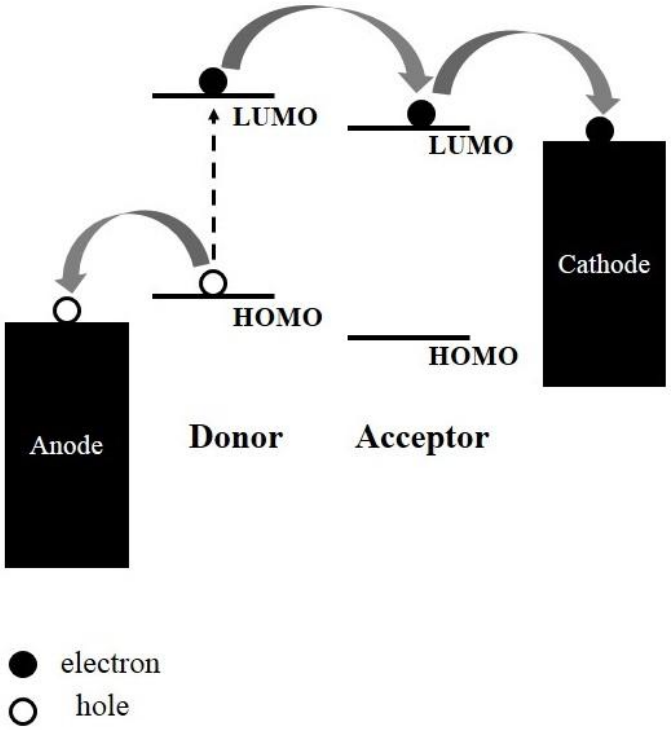

Figure 1. 11. Exciton dissociation in an organic solar cell.

1. 8. Synthesis of Conducting Polymers

Synthesis of conjugated polymers can be achieved via different methods. The two most commonly used methods are the chemical and electrochemical synthesis.

1. 8. 1. Chemical Polymerization

There are different methods that can be applied for the chemical polymerization. A few examples are given below.

Oxidative chemical polymerization takes place in the presence of $FeCl_3$ or other suitable oxidizing agents (Figure 1. 12). [36]

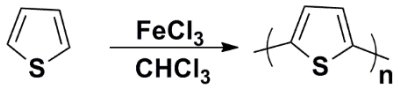

Figure 1. 12. Oxidative chemical polymerization of thiophene with $FeCl_3$.

Suzuki coupling reaction takes place in the presence of palladium (0) complex between an aryl- or vinyl-boronic acid and aryl- or vinyl-halide (Figure 1. 13). [37]

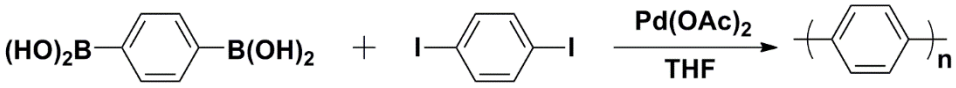

Figure 1. 13. Chemical polymerization via Suzuki coupling reaction.

Stille coupling reaction is the C-C bond formation reaction between stannanes and halides with the help of palladium (II) catalyst (Figure 1. 14). [38]

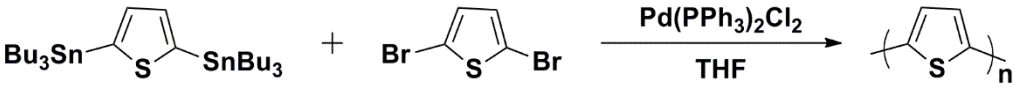

Figure 1. 14. Chemical polymerization via Stille coupling.

Yamamoto coupling is a nickel promoted C-C bond formation reaction through the condensation of dihaloaromatic compounds (Figure 1. 15). [39]

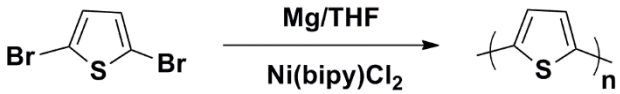

Figure 1. 15. Chemical polymerization via Yamamoto coupling.

1. 8. 2. Electrochemical Polymerization

Electrochemical polymerization is a commonly used method of polymerization since it offers various advantages such as being simple, selective, reproducible, and fast.

Polymerization starts with the electrochemical step which involves the oxidation of the monomer to its radical cation. The electron transfer reaction takes place much faster than the diffusion of the monomer from the bulk to the electrode, therefore; the concentration of radical cations near the electrode surface will be higher. The second step of the polymerization takes place via coupling of monomer radicals. The product of this coupling reaction will form the dimer after the loss of two protons and rearomatization. The third step of the electrochemical polymerization takes place by the oxidation of a dimer since it is more electroactive and hence more easily oxidized than the monomer. Dimer radicals couple with the monomer and forms the trimer and then the same procedure follows until the thiophene chain becomes insoluble in the electrolytic medium and precipitates on the surface of an electrode (Figure 1. 16). [40]

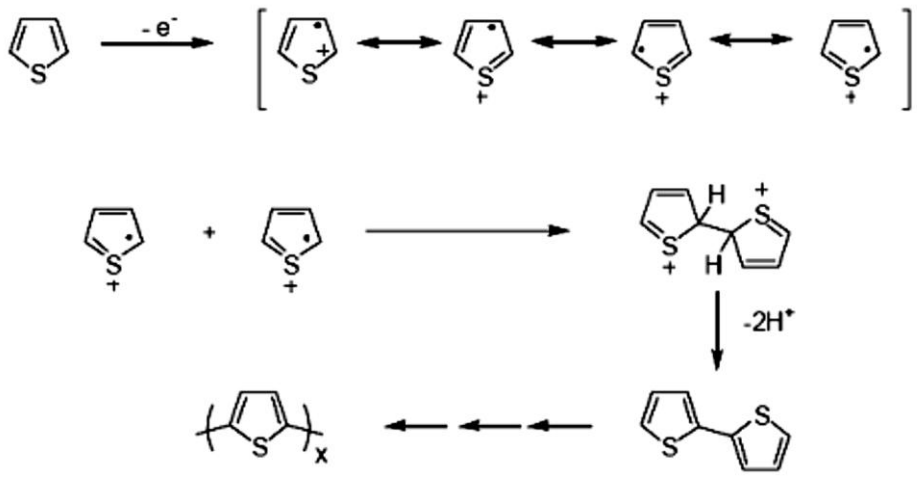

Figure 1. 16. Mechanism for the electrochemical polymerization of thiophene.

CHAPTER 2

EXPERIMENTAL

2. 1. Materials

All reagents were obtained from commercial sources (Aldrich) and used without further purification unless otherwise mentioned. THF was dried over sodium and benzophenone.

2. 2. Equipment

"^{1}H NMR and ^{13}C NMR spectra were recorded in $CDCl_3$ on Bruker Spectrospin Avance DPX-400 Spectrometer with TMS as the internal reference. Electropolymerization was performed in a three electrode cell consisting of an Indium Tin Oxide glass slide (ITO) as the working electrode, platinum wire as the counter electrode, and Ag wire as the pseudo reference electrode under ambient conditions using a Voltalab 50 potentiostat. Before each measurement, argon gas was purged into the solution for five minutes in order to obtain an inert atmosphere. The reference electrode was subsequently calibrated to Fc/Fc^{+} and the band energies were calculated relative to the vacuum level taking the value of SHE as −4.75 eV vs. vacuum. Spectroelectrochemical studies of polymer were carried out using Varian Cary 5000 UV–Vis spectrophotometer. Colorimetry studies were performed via Minolta CS-100 spectrophotometer." [41]

2. 3. Procedure

2. 3. 1. Synthesis

2. 3. 1. 1. Synthesis of 4,7-dibromo-2,1,3-benzothiadiazole

Bromination of benzothiadiazole was performed according to the previously published procedure. [42] Benzothiadiazole (2 g, 14.69 mmol) was dissolved in 36 mL of HBr (47%). 1.6 mL Br_2 and 16 mL HBr (47%) were mixed and added to the reaction mixture drop wise. When the addition was completed the mixture was refluxed for 6 h. The reaction mixture was cooled with an ice-bath and the precipitate was filtered and washed with saturated $NaHSO_3$ in order to remove excess Br_2. Precipitate was dissolved in dichloromethane and washed with water. Organic layer was dried over $MgSO_4$ and solvent was removed under reduced pressure. Product was obtained as a yellow solid with a yield of 95% (4.102 g, 13.96 mmol) (Figure 2. 1). ^{1}H NMR (400 MHz, $CDCl_3$): δ (ppm) 7.65 (s, 2H). ^{13}C NMR (100 MHz, $CDCl_3$): δ (ppm) 152.75, 132.13, 113.70.

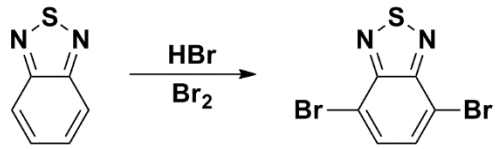

Figure 2. 1. Synthetic route for 4,7-dibromo-2,1,3-benzothiadiazole.

2. 3. 1. 2. Synthesis of 3,6-dibromobenzene-1,2-diamine

Reduction of brominated benzothiadiazole was performed according to the previously published procedure. [43] 4,7-Dibromo-2,1,3-benzothiadiazole (3.38 g, 11.5 mmol) was dissolved in ethanol at 0°C. $NaBH_4$ (8.09 g, 214 mmol) was added slowly. When the addition was completed the reaction mixture was stirred overnight at room temperature. Solvent was evaporated under reduced pressure. The crude product was dissolved in diethyl ether and washed with brine and water respectively. Organic layer was collected and dried over $MgSO_4$. Solvent was removed under reduced pressure and the product was obtained with a yield of 88%. (2.9 g, 10.1 mmol) (Figure 2. 2). ^{1}H NMR (400 MHz, $CDCl_3$): δ (ppm) 6.75 (s, 2H), 3.83 (s,4H). ^{13}C NMR (100 MHz, $CDCl_3$): δ (ppm) 133.74, 123.37, 109.70.

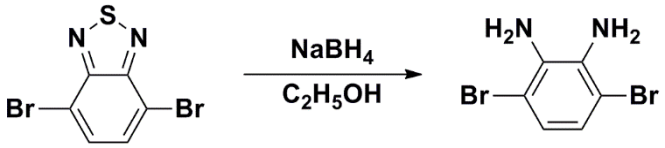

Figure 2. 2. Synthetic route for 3,6-dibromobenzene-1,2-diamine.

2. 3. 1. 3. Synthesis of 4,7-dibromo-4'-(tert-butyl)spiro[benzo[d]imidazole-2,1'-cyclohexane]

"A solution of 3,6-dibromobenzene-1,2-diamine (300 mg, 1.13 mmol), 4-tert-butylcyclohexanone (174 mg, 1.13 mmol) and 8 mL toluene was stirred at 130°C for 24 h under argon atmosphere. The solvent was removed under reduced pressure; crude product was dissolved in 11 mL dichloromethane. 85% activated manganese (IV) oxide (800 mg, 9.16 mmol) was added and stirred at room temperature under argon atmosphere for 4 h. The reaction mixture was filtered, extraction was performed with dichloromethane (80 mL) and the organic phase was dried over $MgSO_4$. Solvent was removed under reduced pressure and the product was purified by silica gel column chromatography. 4,7-Dibromo-4-(tert-butyl)spiro[benzo[d]imidazole-2,1-cyclohexane] was obtained as a yellow solid with a yield of 55% (248.69 mg, 0.62 mmol) (Figure 2. 3)." [41] ^{1}H NMR (400 MHz, $CDCl_3$): δ (ppm) 7.12 (s, 2H), 2.25 (t, 2H), 2.10 (m, 1H), 1.70 (t, 2H), 1.60 (t, 2H), 1.30 (t, 2H), 0.90 (s, 9H). ^{13}C NMR (100 MHz, $CDCl_3$): δ (ppm) 157.00, 156.70, 135.80, 135.60, 119.30, 107.50, 107.50, 107.45, 47.80, 47.85, 47.80, 32.50, 35.80, 35.75, 27.75, 25.70.

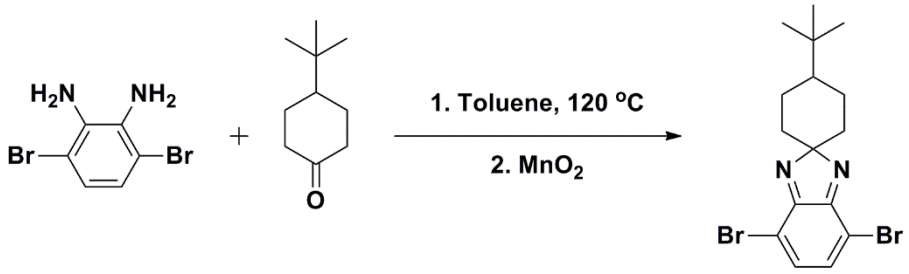

Figure 2. 3. Synthetic route for 4,7-dibromo-4'-(tert-butyl)spiro [benzo[d]imidazole-2,1'-cyclohexane].

2. 3. 1. 4. Synthesis of tributyl(thiophen-2-yl)stannane

Stannylation of thiophene was performed according to the previously published procedure. [44] Thiophene (5.0 g, 59.4 mmol) was dissolved in THF, slowly lithiated with n-buLi (37.2 mL, 59.4 mmol) and stirred for 30 min at -78°C. Then tributyl tinchloride (19.42 g, 59.4 mmol) was added dropwise at -78°C. The solution was stirred overnight at room temperature. Solvent was removed under reduced pressure to give crude product as a brown oily residue with a yield of 80% (17.73 mg, 47.52 mmol) (Figure 2. 4).

Figure 2. 4. Synthetic route for tributyl(thiophen-2-yl)stannane.

2. 3. 1. 5. Synthesis of [2,2'-bithiophen]-5-yltributylstannane

Stannylation of 2,2'-bithiophene was performed according to the previously published procedure. [44] 2,2'-Bithiophene (5.0 g, 30.07 mmol) was dissolved in THF, slowly lithiated with n-buLi (18.83 mL, 30.07 mmol) and stirred for 30 min at -78°C. Then tributyl tinchloride (9.83 g, 30.07 mmol) was added dropwise at -78°C. The solution was stirred overnight at room temperature. Solvent was removed under reduced pressure to give crude product with a yield of 75% (12.18 g, 26.75 mmol) (Figure 2. 5.).

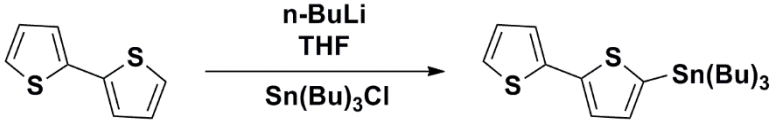

Figure 2. 5. Synthetic route for [2,2'-bithiophen]-5-yltributylstannane.

2. 3. 1. 6. Synthesis of tributyl(thieno[3,2-b]thiophen-2-yl)stannane

"Stannylation of thieno[3,2-b]thiophene was performed according to the previously published procedure. [44] Thieno[3,2-b]thiophene (5.0 g, 35.66 mmol) was dissolved in THF, slowly lithiated with n-buLi (22.33 mL, 35.66 mmol) and stirred for 30 min at -78°C. Then tributyltin chloride (11.66 g, 35.66 mmol) was added drop wise at -78°C. The solution was stirred overnight at room temperature. Solvent was removed under reduced pressure to give crude product with a yield of 78% (11.63 g, 27.81 mmol) (Figure 2. 6)." [41]

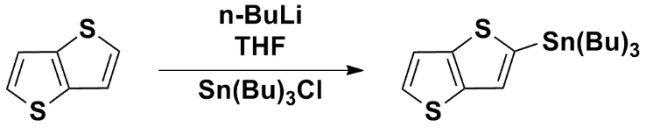

Figure 2. 6. Synthetic route for tributyl(thieno[3,2-b]thiophen-2-yl)stannane.

2. 3. 1. 7. Synthesis of 4'-(tert-butyl)-4,7-di(thiophen-2-yl)spiro[benzo[d]imidazole-2,1'-cyclohexane] (M1)

4,7-Dibromo-4'-(tert-butyl)spiro[benzo[d]imidazole-2,1'-cyclohexane] (200 mg, 0.5 mmol) and tributyl(thiophen-2-yl)stannane (186.59 mg, 0.5 mmol) were dissolved in anhydrous THF (100 mL) and dichlorobis(triphenylphosphine)-palladium(II) (50 mg, 0.045 mmol) was added at room temperature. The mixture was refluxed overnight under an inert atmosphere. The crude product was concentrated under reduced pressure and was purified by column chromatography on silica gel to obtain the product with 76% yield. (154.51 mg, 0.38 mmol) (Figure 2. 7). ^{1}H NMR (400 MHz, $CDCl_3$): δ (ppm) 7.97 (dd, J = 3.7 Hz, 1.1 Hz, 2H), 7.31 (dd, J = 5.1 Hz, 1.0 Hz, 1H), 7.28 (dd, J = 5.1 Hz, 1.1 Hz, 1H), 7.24 (dd, J = 15.3 Hz, 7.3 Hz, 2H), 7.07 - 7.04 (m, 2H), 2.50 (td, J = 13.1 Hz, 3.9 Hz, 2H), 1.95 - 1.79 (m, 4H), 1.35 (tt, J = 12.0 Hz, 3.6 Hz, 1H), 1.23 - 1.17 (m, 2H), 0.94 (s, 9H). ^{13}C NMR (100 MHz, $CDCl_3$): δ (ppm) 157.9, 138.8, 128.5, 127.9, 127.6, 127.0, 126.4, 107.9, 47.7, 33.7, 32.6, 27.7, 26.1.

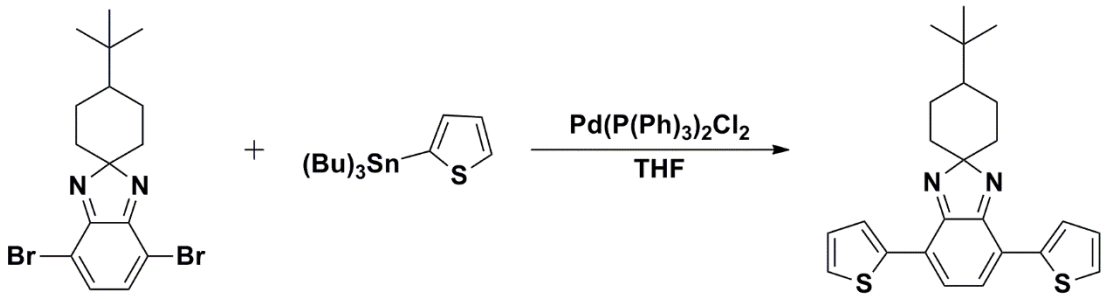

Figure 2. 7. Synthetic route for 4'-(tert-butyl)-4,7-di(thiophen-2-yl)spiro[benzo[d]imidazole-2,1'-cyclohexane].

2. 3. 1. 8. Synthesis of 4,7-di([2,2'-bithiophen]-5-yl)-4'-(tert-butyl)spiro[benzo[d]imidazole-2,1'-cyclohexane] (M2)

4,7-Dibromo-4'-(tert-butyl)spiro[benzo[d]imidazole-2,1'-cyclohexane] (200 mg, 0.5 mmol) and [2,2'-bithiophen]-5-yltributylstannane (227.66 mg, 0.5 mmol) were dissolved in anhydrous THF (100 mL) and dichlorobis(triphenylphosphine)-palladium(II) (50 mg, 0.045 mmol) was added at room temperature. The mixture was refluxed overnight under an inert atmosphere. Solvent was removed under reduced pressure and the crude product was purified by column chromatography on silica gel to obtain the product with 70% yield (199.80 mg, 0.35 mmol) (Figure 2. 8). ^{1}H NMR (400 MHz, $CDCl_3$) δ 7.90 (t, J = 3.4 Hz, 2H), 7.24 – 7.16 (m, 6H), 7.14 (d, J = 3.94 Hz, 1H), 7.12 (d, J = 3.88 Hz, 2H), 1.53 - 1.45 (m, 9H), 0.97 (s, 9H). ^{13}C NMR (100 MHz, $CDCl_3$) δ 137.7, 137.4, 136.6, 136.0, 127.7, 125.0, 124.7, 124.3, 123.9, 123.7, 123.4, 28.9, 27.2, 17.5, 13.6, 10.9.

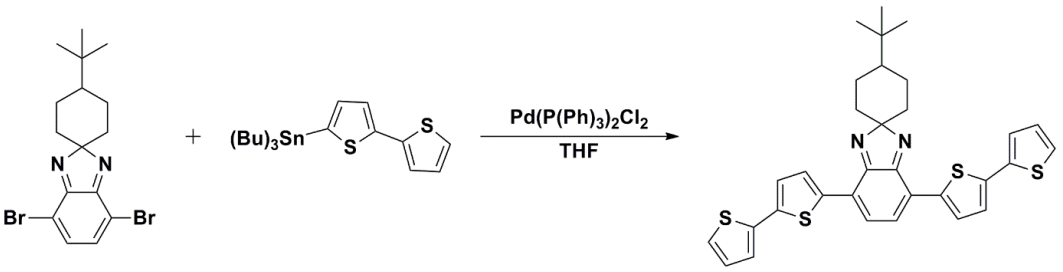

Figure 2. 8. Synthetic route for 4,7-di([2,2'-bithiophen]-5-yl)-4'-(tert-butyl)spiro[benzo[d]imidazole-2,1'-cyclohexane].

2. 3. 1. 9. Synthesis of 4'-(tert-butyl)-4,7-bis(thieno[3,2-b]thiophen-2-yl)spiro[benzo[d]imidazole-2,1'-cyclohexane] (M3)

4,7-Dibromo-4'-(tert-butyl)spiro[benzo[d]imidazole-2,1'-cyclohexane] (200 mg, 0.5 mmol) and tributyl(thieno[3,2-b]thiophen-2-yl)stannane (214.64 mg, 0.5 mmol) were dissolved in anhydrous THF (100 mL) and dichlorobis(triphenylphosphine)-palladium(II) (50 mg, 0.045 mmol) was added at room temperature. The mixture was refluxed overnight under an inert atmosphere. Solvent was removed under reduced pressure and the crude product was purified by column chromatography on silica gel to obtain the product with 78% yield (202.32 mg, 0.39 mmol) (Figure 2. 9). ^{1}H NMR (400 MHz, $CDCl_3$): δ (ppm) 8.34 (s, 2H), 8.32 (s, 2H), 7.36 (d, J = 4.86 Hz, 2H), 7.35 (d, J = 4.3 Hz, 2H), 2.57–2.46 (m, 4H), 1.95–1.81 (m, 4H), 1.39–1.35 (m, 1H), 0.97 (s, 9H). ^{13}C NMR (100 MHz, $CDCl_3$): δ (ppm) 164.4, 127.1, 127.0, 126.7, 126.2, 119.9, 119.4, 118.1, 118.0, 106.5, 46.3, 32.3, 28.2, 26.3, 24.3.

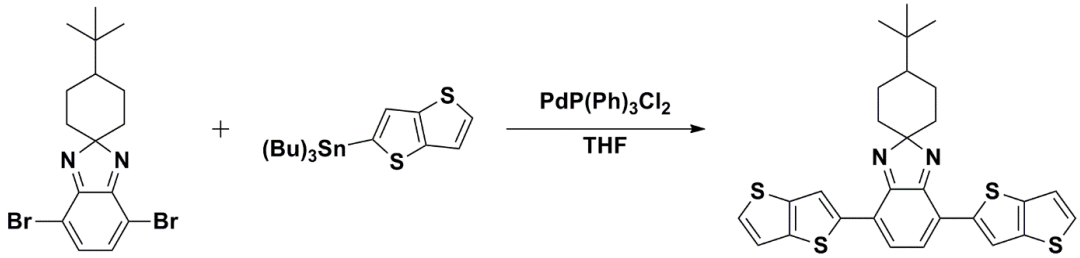

Figure 2. 9. Synthetic route for 4'-(tert-butyl)-4,7-bis(thieno[3,2-b]thiophen-2-yl)spiro[benzo[d]imidazole-2,1'-cyclohexane].

2. 3. 1. 10. Synthesis of 2,7-dibromophenanthrene-9,10-dione

Bromination of phenanthrene-9,10-dione was performed according to the previously described procedure. [45] Phenanthrene-9,10-dione (250 mg, 1.2 mmol) and 10 mL concentrated H_2SO_4 were placed in a flask and stirred at room temperature. N-bromo succinimide (520 mg, 2.92 mmol) was added slowly. After the completion of the addition the reaction mixture was further stirred at room temperature for 3 hours. Then the reaction mixture was poured into crushed ice and stirred for an hour. Orange solid was filtered and dried in oven. 2,7-dibromophenanthrene-9,10-dione was obtained as an orange solid with 90% yield (395 mg, 1.08 mmol) (Figure 2. 10).

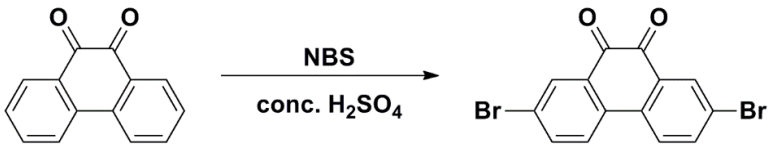

Figure 2. 10. Synthetic route for 2,7-dibromophenanthrene-9,10-dione.

2. 3. 1. 11. Synthesis of 4-(5,10-dibromo-1-phenyl-1H-phenanthro[9,10-d]imidazol-2-yl)phenol

Synthesis of 4-(5,10-dibromo-1-phenyl-1H-phenanthro[9,10-d]imidazol-2-yl)phenol was performed according to the perviously described procedure. [46] 2,7-Dibromophenanthrene-9,10-dione (300 mg, 0.82 mmol), 4-hydroxybenzaldehyde (108.7 mg, 0.89 mmol), aniline (91.27 mg, 0.98 mmol), ammonium acetate (1.25 g, 16.22 mmol), and glacial acetic acid (10 mL) were placed in a flask and refluxed for 3 hours. Then the reaction mixture was poured into water and the solid product was filtered. The crude product was washed with methanol in order to obtain beige solid with 57% yield (255 mg, 0.47 mmol) (Figure 2. 11). ^{1}H NMR (400 MHz, d-DMSO) δ 9.89 (s, 1H), 8.85 (d, J = 9.14 Hz, 1H), 8.84 (d, J = 9.66 Hz, 1H), 8.75 (d, J = 2.21 Hz, 1H), 7.82 (dd, J_1 = 2.25, J_2 = 2.21 Hz, 1H), 7.77 – 7.71 (m, 5H), 7.68 (dd, J_1 = 2.06 Hz, J_2 = 2.05 Hz, 1H), 7.42 (d, J = 8.74 Hz, 2H), 7.05 (d, J = 2.06, 1H), 6.70 – 6.75 (m, 2H).

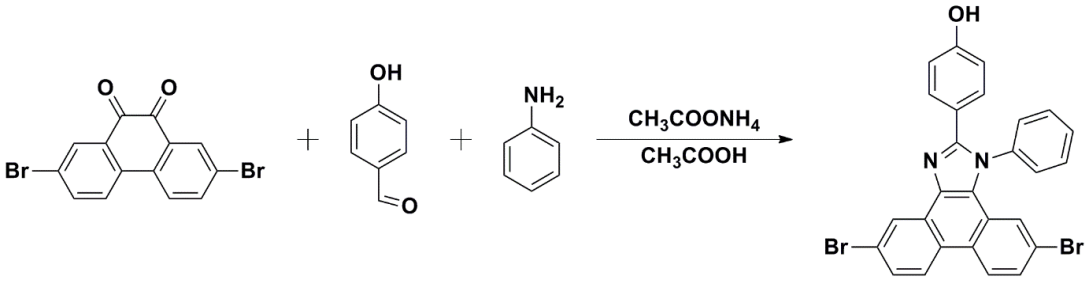

Figure 2. 11. Synthetic route for 4-(5,10-dibromo-1-phenyl-1H-phenanthro[9,10-d]imidazol-2-yl)phenol.

2. 3. 1. 12. Synthesis of 5,10-dibromo-2-(4-(hexadecyloxy)phenyl)-1-phenyl-1H-phenanthro[9,10-d]imidazole

To a mixture of NaH (20 mg, 0.822 mmol) in dimethylformamide (10 mL) at 0°C under an inert atmosphere 4-(5,10-dibromo-1-phenyl-1H-phenanthro[9,10-d]imidazol-2-yl)phenol (373 mg, 0.685 mmol) was added drop wise in dimethylformamide (10 mL). After being stirred at 0°C for 30 minutes $C_{16}H_{33}Br$ was added and stirred at room temperature for 3 hours. Then the reaction mixture was cooled to 0°C and distilled water was added to quench the extra NaH. Organic layer was extracted with ethyl acetate and water. Organic phase was dried over $MgSO_4$ and the solvent was removed under reduced pressure. The solid product was obtained with 80 % yield (421.23 mg, 2.548 mmol) (Figure 2. 12). ^{1}H NMR (400 MHz, d-DMSO) δ 8.93 (d, J = 2.14 Hz, 1H), 8.44 (d, J = 9.06 Hz, 1H), 8.42 (d, J = 8.96 Hz, 1H), 7.65 (dd, J_1 = 2.19 Hz, J_2 = 2.22 Hz, 1H), 7.62 – 7.55 (m, 3H), 7.49 (dd, J_1 = 2.05 Hz, J_2 = 2.05 Hz, 1H), 7.46 – 7.40 (m, 4H), 7.12 (d, J = 2.02 Hz, 2H), 6.76 – 6.72 (m, 2H), 3.87 (t, J = 6.61 Hz, 2H), 1.74 - 1.65 (m, 2H), 1.40 - 1.30 (m, 2H), 1.28 – 1.10 (m, 24H), 0.81 (t, J = 7.02 Hz, 3H).

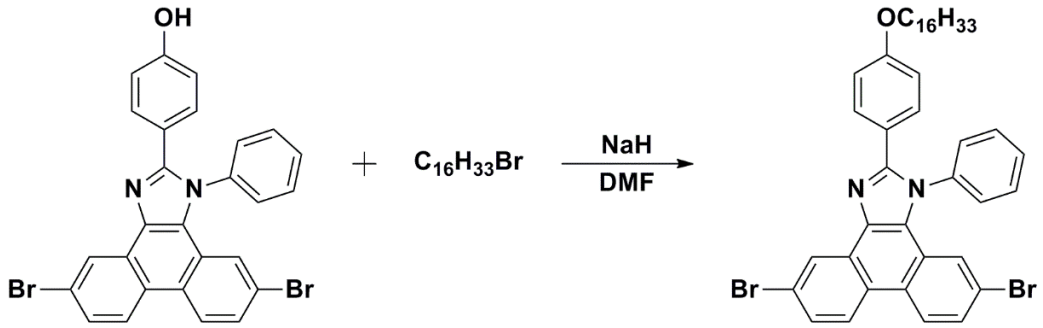

Figure 2. 12. Synthetic route for 5,10-dibromo-2-(4-(hexadecyloxy)phenyl)-1-phenyl-1H-phenanthro[9,10-d]imidazole.

2. 3. 1. 13. Synthesis of poly-(2-(4-(hexadecyloxy)phenyl)-5-methyl-10-(5-methylthiophen-2-yl)-1-phenyl-1H-phenanthro[9,10-d]imidazole) (P1)

5,10-Dibromo-2-(4-(hexadecyloxy)phenyl)-1-phenyl-1H-phenanthro[9,10-d]imidazole (700 mg, 0.91 mmol) and 2,5-bis(tributylstannyl)thiophene (603 mg, 0.91 mmol) were stirred in dry tetrahydrofuran under an inert atmosphere. $Pd(PPh_3)_2Cl_2$ (100 mg, 0.14 mmol) was added and the reaction mixture was refluxed for 2 days. Bromobenzene and tributyl(thiophen-2-yl)stannane were added as end-capper groups. Purification of the resulting polymer was performed using soxhlett extraction with methanol, acetone, and hexane (Figure 2. 13). ^{1}H NMR (400 MHz, $CDCl_3$) δ 8.65 (phenanthrene), 7.48 (phenantrene, benzene attached to the imidazole), 7.19 (-CH_2 pendant group), 6.75 (thiophene), 3.87 (O-CH_2), 1.67 (–CH_2 attached to O-CH_2), 0.18 (–CH_3 pendant group).

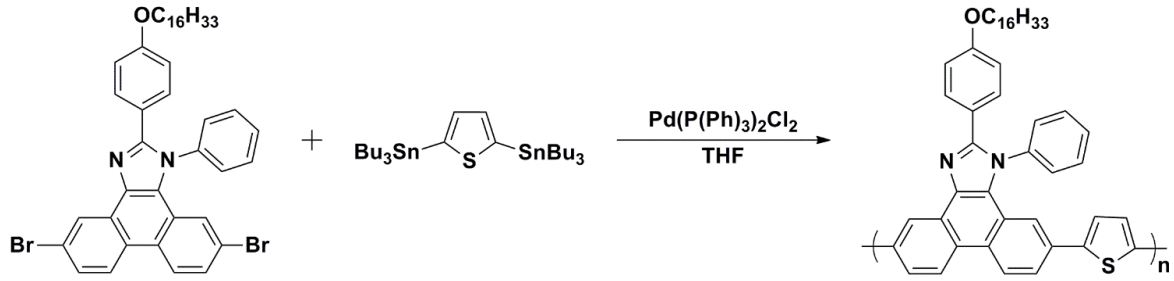

Figure 2. 13. Synthetic route for poly-(2-(4-(hexadecyloxy)phenyl)-5-methyl-10-(5-methylthiophen-2-yl)-1-phenyl-1H-phenanthro[9,10-d]imidazole).

2. 3. 1. 14. Synthesis of poly-(2-(4-(hexadecyloxy)phenyl)-5-methyl-10-(5'-methyl-[2,2'-bithiophen]-5-yl)-1-phenyl-1H-phenanthro[9,10-d]imidazole) (P2)

5,10-Dibromo-2-(4-(hexadecyloxy)phenyl)-1-phenyl-1H-phenanthro[9,10-d]imidazole (600 mg, 0.78 mmol) and 5,5'-bis(tributylstannyl)-2,2'-bithiophene (581 mg, 0.78 mmol) were stirred in dry tetrahydrofuran under an inert atmosphere. $Pd(PPh_3)_2Cl_2$ (100 mg, 0.14 mmol) was added and the reaction mixture was refluxed for 2 days. Bromobenzene and tributyl(thiophen-2-yl)stannane were added as end-capper groups. Purification of the resulting polymer was performed using soxhlett extraction with methanol, acetone, and hexane (Figure 2. 14). ^{1}H NMR (400 MHz, $CDCl_3$) δ 8.67 (phenanthrene), 7.60 + 7.59 + 7.45 + 7.41 (phenanthrene, thiophene), 6.72 (thiophene), 3.82 (O-CH_2), 1.52 (-CH_2 pendant group), 1.32 (-CH_2 pendant group), 0.81 (-CH_3 pendant group).

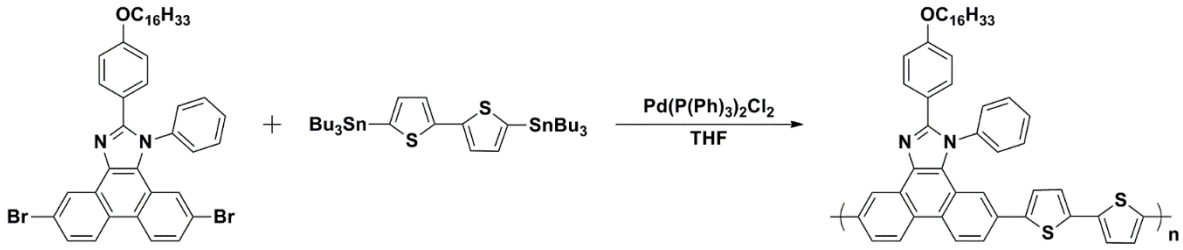

Figure 2. 14. Synthetic route for poly-(2-(4-(hexadecyloxy)phenyl)-5-methyl-10-(5'-methyl-[2,2'-bithiophen]-5-yl)-1-phenyl-1H-phenanthro[9,10-d]imidazole).

CHAPTER 3

RESULTS AND DISCUSSION

3. 1. Synthesis of 4'-(tert-butyl)-4,7-di(thiophen-2-yl)spiro[benzo[d]imidazole-2,1'-cyclohexane] (M1)

Initially, benzothiadiazole was brominated and then reduced to the corresponding 3,6-dibromobenzene-1,2-diamine using $NaBH_4$ as the reducing agent. Condensation reaction between 3,6-dibromobenzene-1,2-diamine and 4-hydroxybenzaldehyde was performed to afford 4,7-dibromo-4'-(tert-butyl)spiro[benzo[d]imidazole-2'-cyclohexane]. Thiophene was converted to lithium salt in the presence of n-BuLi and the salt was reacted with $SnBu_3Cl$ at -78°C under an inert atmosphere to yield tributyl(thiophen-2-yl)stannane. Finally, 4,7-dibromo-4'-(tert-butyl)spiro[benzo[d]imidazole-2'-cyclohexane] was coupled with tributyl(thiophen-2-yl)stannane via Stille coupling reaction and 4'-(tert-butyl)-4,7-di(thiophen-2-yl)spiro[benzo[d]imidazole-2,1'-cyclohexane] were synthesized in good yields.

3. 2. Electrochemistry of 4'-(tert-butyl)-4,7-di(thiophen-2-yl)spiro[benzo[d]imidazole-2,1'-cyclohexane] (M1)

Electrochemical polymerization of the monomer was performed via cyclic voltammetry (CV) in order to probe redox behaviors and determine highest occupied molecular orbital (HOMO) and lowest unoccupied molecular orbital (LUMO) of the corresponding polymer.

Electrochemical polymerization of **M1** was performed on ITO electrode in 0.1 M $TBAPF_6$ in acetonitrile (ACN) /dichloromethane (CH_2Cl_2) (95/5, v/v) solution by applying potentials between 0 V and 1.2 V at a scan rate of 100 mV s^{-1}. Monomer oxidation was observed at 1.1 V in the first anodic cycle representing the formation of the radical cations leading to the synthesis of polymer on the working electrode surface. Electrochemical polymerization of **M1** was performed successfully (Figure 3. 1.).

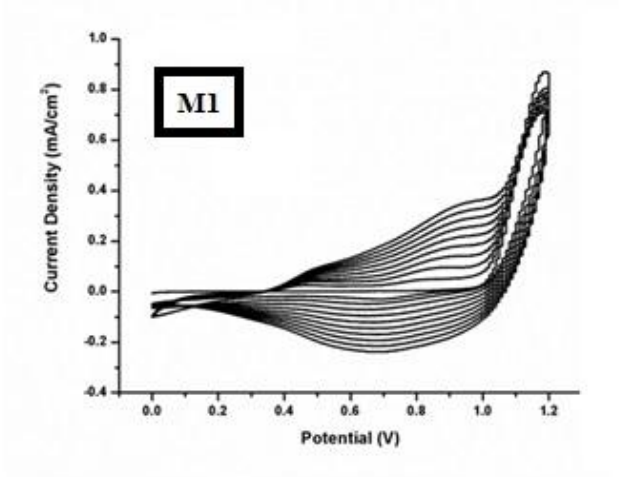

Figure 3. 1. Electrochemical polymerization of **M1**.

Resulting polymer was studied by CV in monomer free solution in order to examine both p-type and n-type doping properties of the polymer (Figure 3. 2). It is important that electrochemical polymer of **M1** (**EPM1**) is ambipolar, in other words revealing both p-doping and n-doping ability. Well-defined two reversible redox couples were observed during p-doping at 0.57 V/0.37 V and 1.06 V/0.87 V and during n-doping at -1.3 V/-1.0 V for **EPM1**. A material exhibiting both n- and p-doping processes at the same time is a good candidate for battery, super capacitor and light-emitting diode applications.

HOMO and LUMO energy levels of the polymer were calculated from the oxidation and reduction onset potentials. Corresponding HOMO and LUMO energy levels of **EPM1** were determined to be –5.17 and –4.39 eV with the corresponding electrochemical band gap (E_g^{ec}) of 0.78 eV.

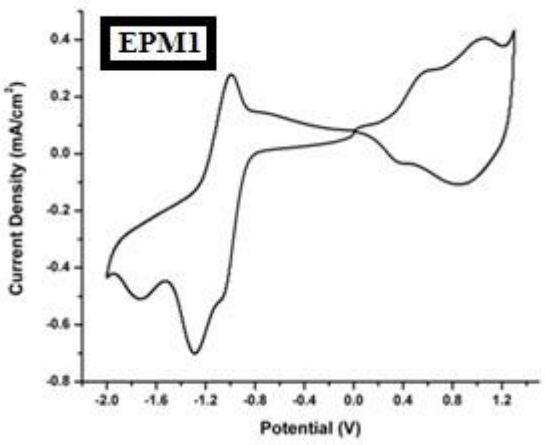

Figure 3. 2. CV of **EPM1** in monomer free environment.

3. 3. Electronic and optical studies of EPM1

Electro-optical properties of the polymer film on ITO were observed by monitoring in situ UV-Vis-NIR spectra in a monomer free medium. Before starting stepwise oxidation, in order to remove any trapped charge and dopant ion caused during electrochemical polymerization, polymer film on ITO was reduced to its neutral state. After taking the neutral film absorption, changes in the absorption spectra under a variety of voltage pulses were recorded (Figure 3. 3). Before applying any potential, two absorption maxima were observed for **EPM1** in neutral state that was attributed to π–π* transition localized on donor or acceptor and intramolecular charge transfer inherent to the donor-acceptor system. Optical band gap (E_g^{op}) was calculated from the onset of lowest energy π–π* transitions as 1.19 eV for **EPM1**.

During the stepwise oxidation of the the polymer, neutral state absorption decreases, new absorption bands appear in NIR region which were attributed to the formation of charge carriers (polaron, bipolaron bands). **EPM1** was blue in its neutral state with neutral state absorption maxima at 380 nm and 640 nm and after stepwise oxidation transmissive blue color was observed, where it reveals light orange color in n-doped state (Figure 3. 4.). In the highly oxidized state a continuous absorption band through the NIR tailing into the visible region of the spectrum causing transmissive blue color.

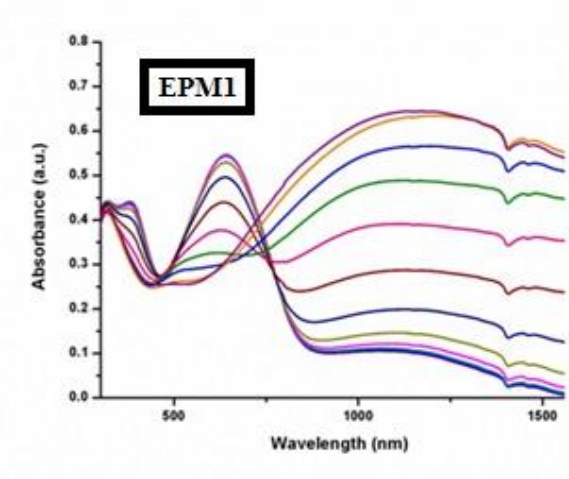

Figure 3. 3. Spectroelectrochemical studies of **EPM1**.

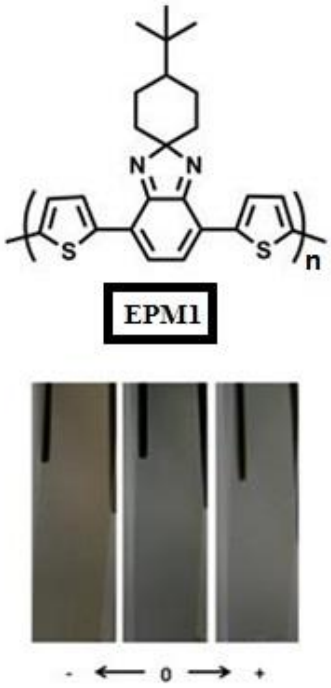

Figure 3. 4. Structure and colors of EPM1 during redox process.

3. 4. Kinetic studies of EPM1

Electrochromic switching studies were carried out to monitor optical contrast and switching time by stepping the potential between reduced and oxidized states with 5 s time intervals (Figure 3. 5). Kinetic measurements were performed in a monomer free ACN / $TBAPF_6$ solvent–electrolyte couple for **EPM1**. The specific wavelengths for these scans were determined from the maximum absorbance in the spectrum of the polymer film.

EPM1 showed 53 % transmittance change upon doping/de-doping process at 1200 nm and 22 % at 640 nm (Figure 3. 5). Switching times were calculated as 1.1 s and 1.0 s at corresponding wavelengths.

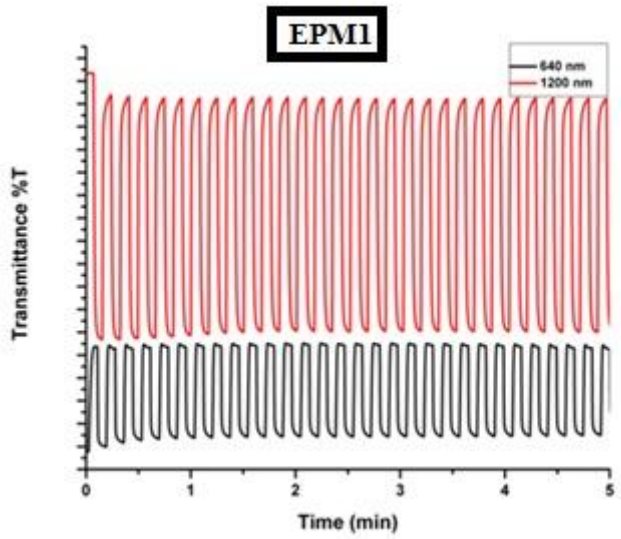

Figure 3. 5. Kinetic studies of **EPM1** at 640 nm and 1200 nm.

3. 5. Synthesis of 4,7-di([2,2'-bithiophen]-5-yl)-4'-(tert-butyl)spiro[benzo[d]imidazole-2,1'-cyclohexane (M2)

Synthesis of M2 is similar to the one for the synthesis of M1 except 4,7-dibromo-4'-(tert-butyl)spiro[benzo[d]imidazole-2'-cyclohexane] was coupled with [2,2'-bithiophen]-5-yltributylstannane to yield 4,7-di([2,2'-bithiophen]-5-yl)-4'-(tert-butyl)spiro[benzo[d]imidazole-2,1'-cyclohexane].

3. 6. Electrochemistry of 4,7-di([2,2'-bithiophen]-5-yl)-4'-(tert-butyl)spiro[benzo[d]imidazole-2,1'-cyclohexane (M2)

Electrochemical polymerization of the monomer was performed via cyclic voltammetry (CV) in order to probe redox behaviors and determine highest occupied molecular orbital (HOMO) and lowest unoccupied molecular orbital (LUMO) of the corresponding polymer.

Electrochemical polymerization of **M2** was not achieved via a common procedure. After trying different solvent-supporting electrolyte couples, electrochemical polymerization of **M2** was carried out in 0.1M propylene carbonate (PC) solution containing LiClO4/$NaClO_4$ via applying potentials between -0.3 V and 1.5 V at a scan rate of 100 mV s^{-1} (Figure 3. 6.).

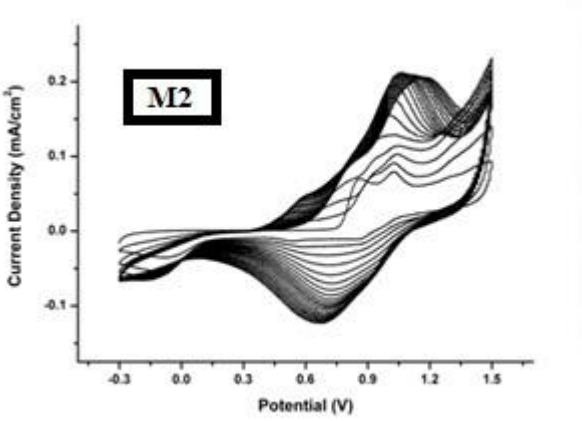

Figure 3. 6. Electrochemical polymerization of **M2**.

Resulting polymer was studied with CV in a monomer free solution in order to examine both p-type and n-type doping properties of the polymer (Figure 3. 7). In a monomer free medium, CV of electrochemically polymerized M2 (**EPM2)** revealed p-doping property where a reversible redox couple at 1.03 V/ 0.64 V versus Ag wire pseudo reference electrode was observed.

HOMO and LUMO energy levels of the polymer were calculated from the oxidation and reduction onset potentials. Since **EPM2** was only p-dopable, LUMO energy level was not calculated from CV. HOMO energy level of the **EPM2** was determined as -5.56 eV and relative LUMO energy level of the **EPM2** was estimated from HOMO and optical band gap derived from the absorption edge in the absorption spectrum of the polymer and determined as - 4.41 eV.

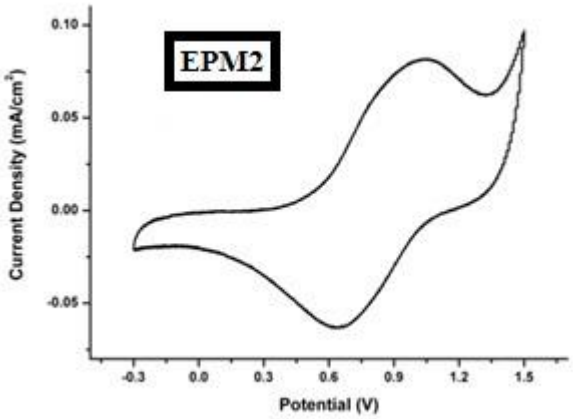

Figure 3. 7. CV of **EPM2** in monomer free environment.

3. 7. Electronic and optical studies of EPM2

Electro-optical properties of the polymer film on ITO were observed by monitoring in situ UV-Vis-NIR spectrum in a monomer free medium. Before starting stepwise oxidation, in order to remove any trapped charge and dopant ion caused during electrochemical polymerization, polymer film on ITO was reduced to its neutral state. After taking the neutral film absorption, changes in the absorption spectrum under a variety of voltage pulses were recorded (Figure 3. 8). Before applying any potential, two absorption maxima were observed for **EPM2** in neutral state that was attributed to π–π* transition localized on donor or acceptor and intramolecular charge transfer inherent to the donor-acceptor system. Optical band gap (E_g^{op}) was calculated from the onset of lowest energy π–π* transitions as 1.15 eV for **EPM2**.

During the stepwise oxidation of the the polymer, neutral state absorption decreases, new absorption bands appear in NIR region which were attributed to the formation of charge carriers (polaron, bipolaron bands). The absorption maxima of **EPM2** were 457 nm and 645 nm which were red shifted compared to the **EPM1**. This shift in the absorption maxima was ascribed to the strength of donor unit and increasing conjugation.

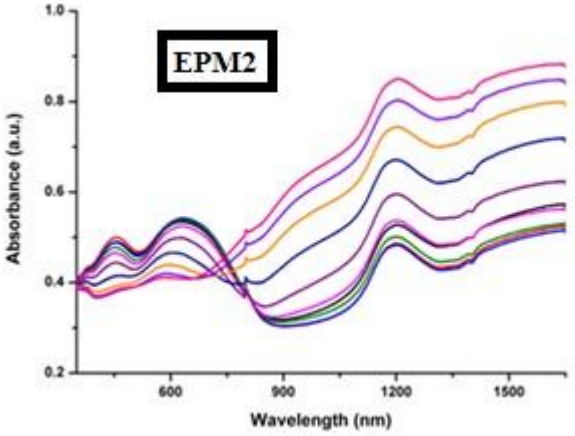

Figure 3. 8. Spectroelectrochemical studies of **EPM2**.

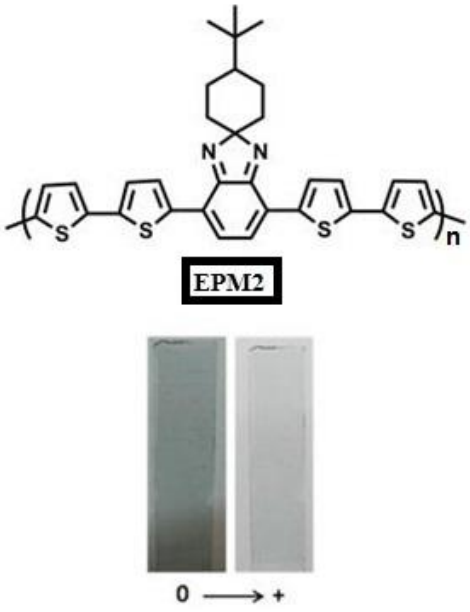

Figure 3. 9. Structure and colors of **EPM2** during redox process.

3. 8. Kinetic studies of EPM2

Electrochromic switching studies were carried out to monitor optical contrast and switching time by stepping the potential between reduced and oxidized states with 5 s time intervals (Figure 3. 10). Kinetic measurements were performed in a monomer free PC/ $TBAPF_6$ system for **EPM2**. The specific wavelengths for these scans were determined from the maximum absorbance in the spectrum of polymer film.
EPM2 revealed 4 % transmittance at 1200 nm, 3 % transmittance at 950 nm and 1 % transmittance at 640 nm. Due to these low percent transmittance changes, corresponding switching times were not calculated. **EPM2** exhibited blue in its neutral state and higher optical transparency compared to **EPM1**.

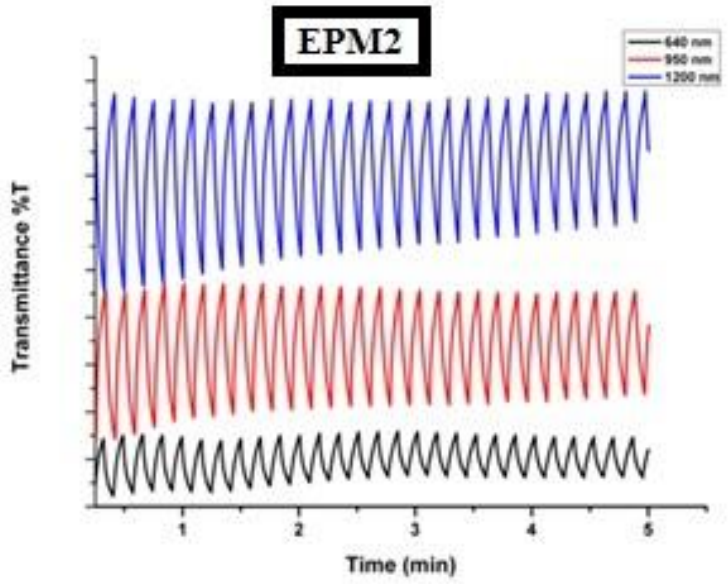

Figure 3. 10. Kinetic studies of **EPM2** at 640 nm, 950 nm, and 1200 nm.

3. 9. Synthesis of 4'-(tert-butyl)-4,7-bis(thieno[3,2-b]thiophen-2-yl)spiro[benzo[d]imidazole-2,1'-cyclohexane] (M3)

Synthesis of **M3** is similar to the synthesis of **M1** and **M2**. The Stille coupling reaction of 4,7-dibromo-4'-(tert-butyl)spiro[benzo[d]imidazole-2'-cyclohexane] with tributyl(thieno[3,2-b]thiophen-2-yl)stannane was performed in dry THF with $Pd(PPh_3)_2Cl_2$ as the catalysts and 4'-tert-butyl-4,7-di(thieno[3,2-b]thiophen-2-yl)spiro[benzo[d]imidazole-2,1'-cyclohexane] **(M3)** was synthesized in good yield.

3. 10. Electrochemistry of 4'-(tert-butyl)-4,7-bis(thieno[3,2-b]thiophen-2-yl)spiro[benzo[d]imidazole-2,1'-cyclohexane] (M3)

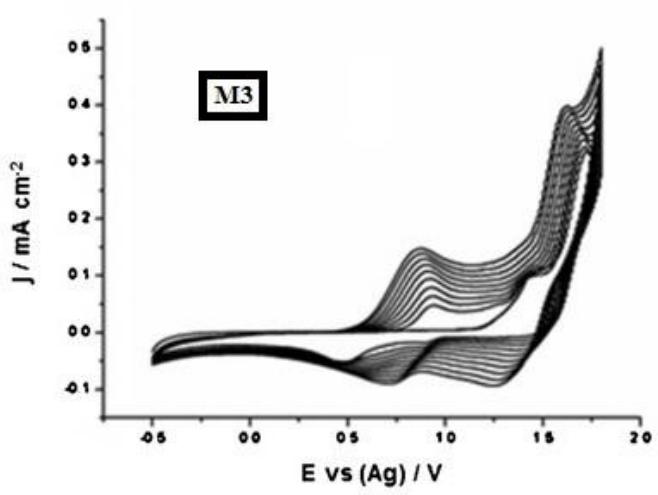

Figure 3. 11. Electrochemical polymerization of **M3**.

Electrochemical studies were performed in three electrode cells using ITO coated glass slide as the working, Pt wire as the counter and Ag wire (0.3 V vs. Fc/Fc^{+}) as the pseudo reference electrodes. The electrochemical polymerization was carried out in a 0.1 M $TBAPF_6$/DCM solution containing 0.01 M monomer by sweeping the potential between −0.5 V and 1.8 V (Figure 3. 11). Although monomer bears pendant 4-tert-butylcyclohexanone unit, **M3** was slightly soluble in acetonitrile due to fused structure of thieno[3,2- b]thiophene, thus dichloromethane was used as the solvent to acquire sufficient solubility. In the first cycle of polymerization, an irreversible oxidation peak at 1.43 V was observed indicating monomer oxidation. The representative electrochemical growth during polymerization indicated formation of corresponding polymer film on the working electrode. p- and n-type doping studies of resulted polymer (**EPM3**) revealed two pseudo reversible oxidation couples, whereas one irreversible reduction peak was observed at −1.61 V (Figure 3. 12). HOMO and LUMO energy levels of **EPM3** were estimated from onset of the oxidation and reduction potentials as −5.73 and −3.79 eV, respectively. [41]

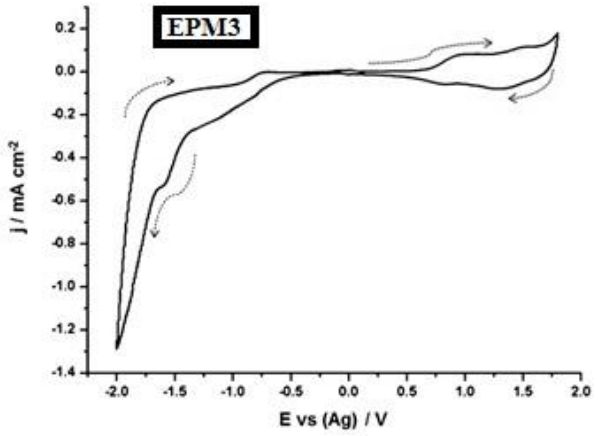

Figure 3. 12. CV of **EPM3** in monomer free environment.

3. 11. Electronic and Optical Studies of EPM3

"Optical studies were carried out to investigate the degree of transparency of **EPM3**. Using UV–Vis–NIR spectrophotometer optical studies were performed in a monomer free, 0.1 M $TBAPF_6$/DCM solution via increasing the applied potential from + 0.0 V to +1.80 V. In its neutral state, the polymer revealed no absorption in the visible region (Figure 3. 13). Optical band gap of the polymer was determined from the π–π* transition onset and found as 1.60 eV for **EPM3**. During the in situ doping, polarons and bipolarons were formed around 1200 nm. Optical contrast tests were performed to investigate the percent transmittance changes during switching from fully neutral and oxidized states of the polymer within 5 s time intervals at the wavelength (555 nm) where human eye is highly sensitive." [41]

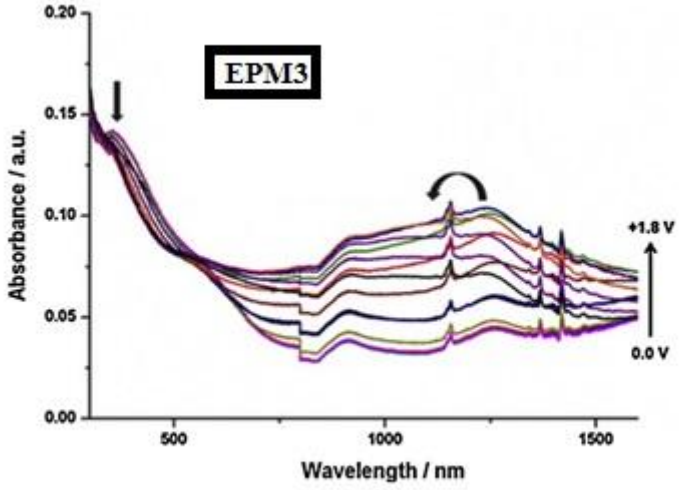

Figure 3. 13. Spectroelectrochemical studies of **EPM3**.

3. 12. Kinetic Studies of EPM3

"The material to be used as a hole injection layer for photovoltaic applications has to be transparent in the oxidized form which is provided by this polymer. PEDOT-PSS retained optical transparency over 75% and 85% in the visible range whereas in the case of **EPM3**, it showed around 95% transmittance in its oxidized state (Figure 3. 15) which is a superior to PEDOT. Furthermore, electrochromic materials that are used in electrochromic device fabrication generally contain anodically or cathodically coloring polymers and a transparent state is desired for an electrochromic device. In our case **EPM3** showed high optical transparency in both redox states and there is no color seen in the intermediate state (Figure 3. 14). We believe that such a transition from a colorless neutral state to a colorless oxidized state is due to the fact that as the polymer is oxidized the backbone is transformed from a twisted conformation to a planar structure, allowing the charge carriers to become delocalized. This causes a shift in the bipolaron transition to NIR region which in return allows the polymer to reveal a second colorless state." [41]

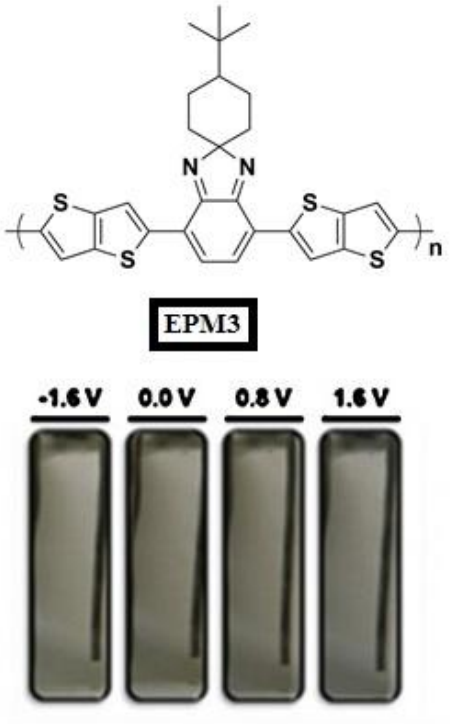

Figure 3. 14. Structure and colors of **EPM3** during redox process.

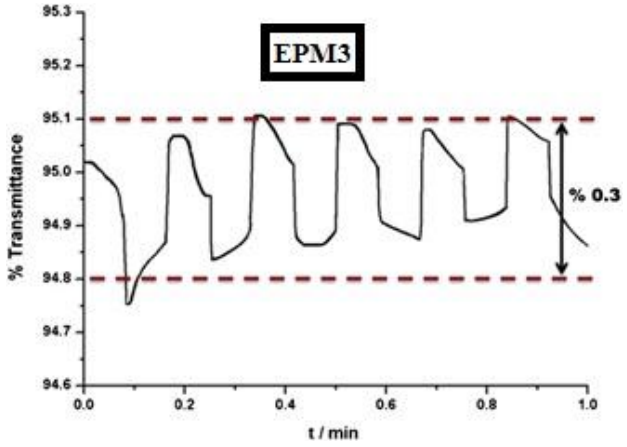

Figure 3. 15. Kinetic study of **EPM3** at 555 nm.

3. 13. Synthesis of poly-(2-(4-(hexadecyloxy)phenyl)-5-methyl-10-(5-methylthiophen-2-yl)-1-phenyl-1H-phenanthro[9,10-d]imidazole) (P1)

Phenanthrene-9,10-dione was brominated using N-bromosuccinimide and sulfuric acid. Brominated product was reacted with 4-hydroxybenzaldehyde, aniline and ammonium acetate in glacial acetic acid to produce 4-(5,10-dibromo-1-phenyl-1H-phenanthro[9,10-d]imidazol-2-yl)phenol. Alkylation of 4-(5,10-dibromo-1-phenyl-1H-phenanthro[9,10-d]imidazol-2-yl)phenol yields the acceptor unit. Polymerization was performed via Stille coupling reaction with Pd(II) catalyst. Bromobenzene and tributyl(thiophen-2-yl)stannane was used as end-capper groups. Soxhlett extraction with methanol, acetone, and hexane was performed in order to purify the produced polymer.

3. 14. Electrochemistry of poly-(2-(4-(hexadecyloxy)phenyl)-5-methyl-10-(5-methylthiophen-2-yl)-1-phenyl-1H-phenanthro[9,10-d]imidazole) (P1)

Electrochemical studies of **P1** were performed in three electrode cells using ITO coated glass slide as the working, Pt wire as the counter and Ag wire (0.3 V vs. Fc/Fc^{+}) as the pseudo reference electrodes. The polymer was spray coated on ITO surface from the solution in chloroform.

P1 revealed p-doping property with a reversible redox couple at 1.45 V/ 1.03 V versus Ag wire pseudo reference electrode. HOMO level of **P1** was calculated by using the onset of oxidation potential as -5.87 eV. Since **P1** was not n-dopable LUMO energy level cannot be calculated from the cyclic voltammogram (Figure 3. 16).

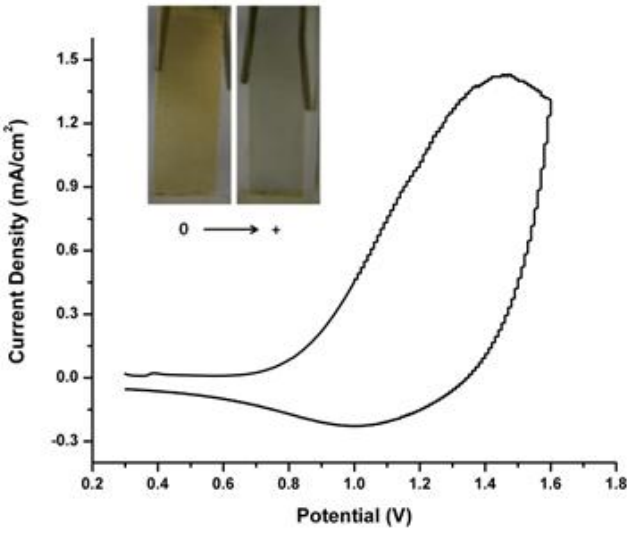

Figure 3. 16. Cyclic voltammogram of **P1**.

3. 15. Optical Studies of poly-(2-(4-(hexadecyloxy)phenyl)-5-methyl-10-(5-methylthiophen-2-yl)-1-phenyl-1H-phenanthro[9,10-d]imidazole) (P1)

Spectroelectrochemical studies of P1 was performed in order to see the absorption spectrum of the polymer upon stepwise oxidation (Figure 3. 17). Using UV–Vis–NIR spectrophotometer optical studies were performed in a 0.1 M $TBAPF_6$/ACN solution via increasing the applied potential from + 0.6 V to +1.4 V.

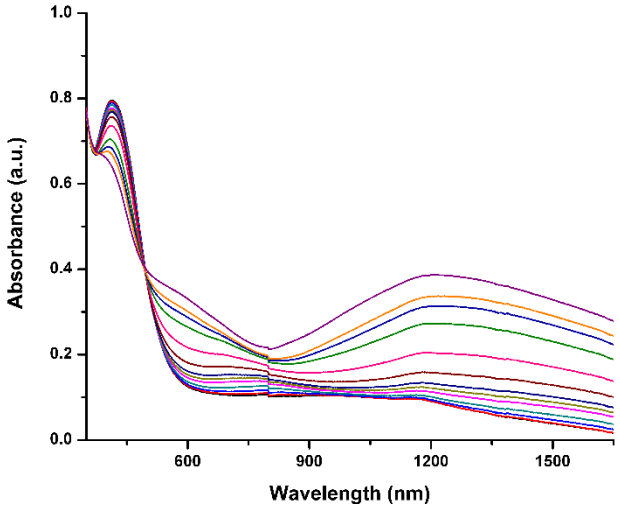

Figure 3. 17. Spectroelectrochemical studies of **P1**.

3. 16. Kinetic Studies of poly-(2-(4-(hexadecyloxy)phenyl)-5-methyl-10-(5-methylthiophen-2-yl)-1-phenyl-1H-phenanthro[9,10-d]imidazole) (P1)

Electrochromic switching studies were carried out to monitor optical contrast and switching time by stepping the potential between reduced and oxidized states with 5 s time intervals (Figure 3. 18). The specific wavelengths for these scans were determined from the maximum absorbance in the spectrum of polymer film. P1 revealed 8 % transmittance at 1250 nm and 3.4s switching time.

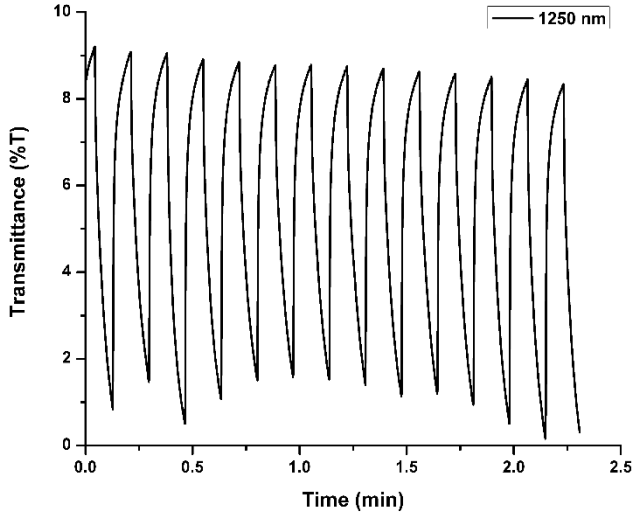

Figure 3. 18. Kinetic studies of **P1**.

3. 17. Synthesis of poly-(2-(4-(hexadecyloxy)phenyl)-5-methyl-10-(5'-methyl-[2,2'-bithiophen]-5-yl)-1-phenyl-1H-phenanthro[9,10-d]imidazole) (P2)

Synthesis of **P2** is similar to the synthesis of **P1** except the acceptor unit was coupled with bithiophene group.

3. 18. Electrochemistry of poly-(2-(4-(hexadecyloxy)phenyl)-5-methyl-10-(5'-methyl-[2,2'-bithiophen]-5-yl)-1-phenyl-1H-phenanthro[9,10-d]imidazole) (P2)

Electrochemical studies of **P2** were performed in three electrode cells using ITO coated glass slide as the working, Pt wire as the counter and Ag wire (0.3 V vs. Fc/Fc^{+}) as the pseudo reference electrodes. The polymer was spray coated on ITO surface from the solution.

P2 revealed 2 reversible redox couple at 0.95 V / 0.62 V and 1.22 V / 0.87 V versus Ag wire pseudo reference electrode. HOMO level of **P2** was calculated using the onset of first oxidation potential as -5.64 eV. Since **P2** was not n-dopable LUMO energy level cannot be calculated from the cyclic voltammogram (Figure 3. 19).

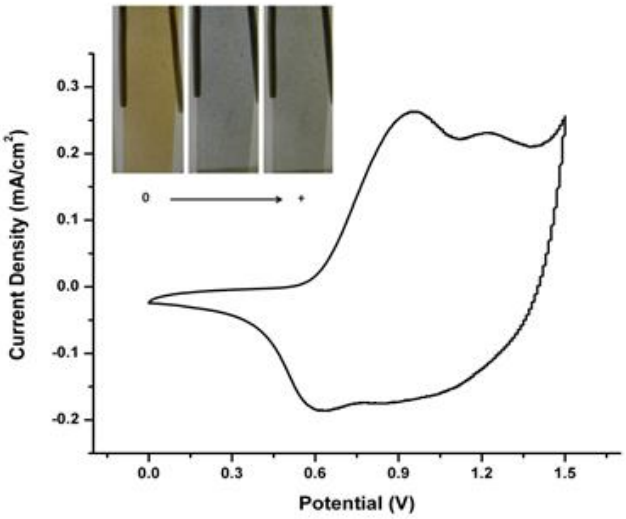

Figure 3. 19. Cyclic voltammogram of **P2**.

3. 19. Optical Studies of poly-(2-(4-(hexadecyloxy)phenyl)-5-methyl-10-(5'-methyl-[2,2'-bithiophen]-5-yl)-1-phenyl-1H-phenanthro[9,10-d]imidazole) (P2)

Spectroelectrochemical studies of P2 was performed in order to see the absorption spectrum of the polymer upon stepwise oxidation (Figure 3. 20). Using UV–Vis–NIR spectrophotometer optical studies were performed in a 0.1 M $TBAPF_6$/ACN solution via increasing the applied potential from + 0.6 V to +1.2 V.

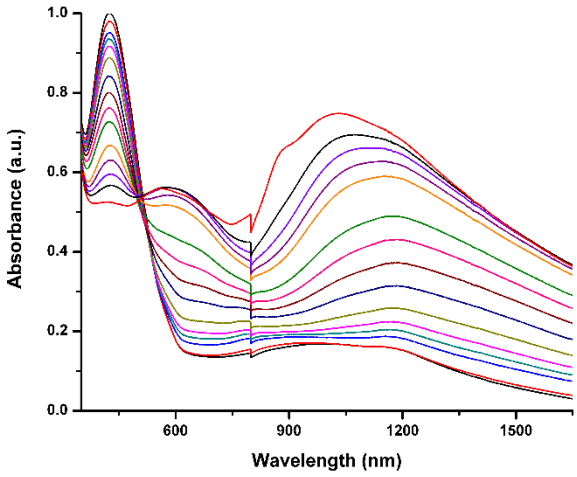

Figure 3. 20. Spectroelectrochemical studies of **P2**.

3. 20. Kinetic Studies of P2

Electrochromic switching studies were carried out to monitor optical contrast and switching time by stepping the potential between reduced and oxidized states with 5 s time intervals (Figure 3. 21). The specific wavelengths for these scans were determined from the maximum absorbance in the spectrum of polymer film. **P2** revealed 46 % transmittance at 1085 nm, 16 % transmittance at 620 nm, and 28 % transmittance at 425 nm. Corresponding switching times are 1.2, 1.1, 1.7 s relatively.

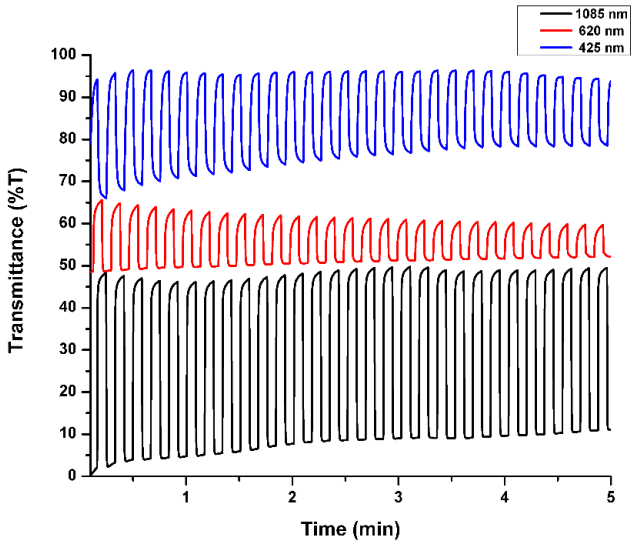

Figure 3. 21. Kinetic studies of **P2**.

CHAPTER 4

CONCLUSION

Three novel monomers were synthesized and electrochemically polymerized on ITO coated glass surface. Electrochemical, spectroelectrochemical, and kinetic studies were performed.

For **EPM1** two reversible redox couples were observed during p-doping at 0.57 V / 0.37 V and 1.06 V / 0.87 V and during n-doping at -1.3 V / -1.0 V. Corresponding HOMO and LUMO energy levels of **EPM1** were determined to be –5.17 and –4.39 eV with the corresponding electrochemical band gap (E_g^{ec}) of 0.78 eV. Optical band gap (E_g^{op}) of **EPM1** was calculated from the onset of lowest energy π–π* transitions as 1.19 eV. **EPM1** showed 53 % transmittance change upon doping/de-doping process at 1200 nm and 22 % at 640 nm. Switching times were calculated as 1.1 s and 1.0 s at corresponding wavelengths.

EPM2 revealed p-doping property where a reversible redox couple at 1.03 V / 0.64 V versus Ag wire pseudo reference electrode. HOMO energy level of the **EPM2** was determined as -5.56 eV and relative LUMO energy level of the **EPM2** was estimated from HOMO and optical band gap derived from the absorption edge in the absorption spectrum of the polymer and determined as - 4.41 eV. Optical band gap (E_g^{op}) was calculated from the onset of lowest energy π–π* transitions as 1.15 eV for **EPM2**. **EPM2** revealed 4 % transmittance at 1200 nm, 3 % transmittance at 950 nm and 1 % transmittance at 640 nm.

"EPM3 revealed two pseudo reversible oxidation couples, whereas one irreversible reduction peak was observed at −1.61 V. HOMO and LUMO energy levels of **EPM3** were estimated from onset of the oxidation and reduction potentials as −5.73 and −3.79 eV, respectively. Optical band gap of the polymer was determined from the π–π* transition onset and found as 1.60 eV for **EPM3**." [41]

Two new polymers were synthesized chemically and spray coated on ITO surface. Their electrochemical, spectroelectrochemical, and kinetic studies were performed.

P1 revealed p-doping property with a reversible redox couple at 1.45 V/ 1.03 V versus Ag wire pseudo reference electrode. HOMO level of **P1** was calculated using the onset of oxidation potential as -5.87 eV. **P1** revealed 8 % transmittance at 1250 nm and 3.4s switching time.

P2 revealed 2 reversible redox couple at 0.95 V / 0.62 V and 1.22 V / 0.87 V versus Ag wire pseudo reference electrode. HOMO level of **P2** was calculated by using the onset of first oxidation potential as -5.64 eV. **P2** revealed 46 % transmittance at 1085 nm, 16 % transmittance at 620 nm, and 28 % transmittance at 425 nm. Corresponding switching times are 1.2, 1.1, 1.7s relatively.

The optical band gaps of polymers are 2.15 eV for **P1** and 2.02 eV for **P2**. The relatively low band gap of **P2** can be attributed to increased conjugation in the polymer backbone due to the presence of bithiophene unit since the increased conjugation leads to lower band gap.

REFERENCES

1. Staudinger, H. *Ber. dtsch. Chem. Ges. A/B*, **1920**, *53*, 1073.
2. Greve, H. H. *Ullmann's Encyclopedia of Industrial Chemistry*, **2000**.
3. US Patent 2130523 "Linear polyamides suitable for spinning into strong pliable fibers" issued September 20, **1938**.
4. US Patent 3819587 "Wholly aromatic carbocyclic polycarbonate fiber having orientation angle of less than about 45 degrees" issued June 25, **1974**.
5. Shirakawa H., Louis E. J., MacDiarmid A.G., Chiang C.K., Heeger A. J., *J. Chem. Soc. Chem. Commun*, **1977**, *16*, 578.
6. Bohr, N. *Atomic theory and the description of nature*, **1934**.
7. Jones J. L., *Trans. Faraday Soc.*, **1929**, *25*, 668.
8. Salzner U., Lagowski J.B., Pickup P.G., Poirier R.A., *Synthetic Metals*, **1998**, *96*, 177.
9. Mullekom H.A.M., Vekemans J.A.J.M., Havinga E.E., Meijer E.W., *Materials Science and Engineering*, **2001**, *32*, 1.
10. Reddinger J. I., Reynolds J. R., *Advances in Polymer Science* **1999**, *45*, 59.
11. Hoffmann R., *Angew. Chem. Int. Ed.*, **1987**, *26*, 846.
12. Heeger A. J., *J. Phys. Chem. B*, **2001**, *105*, 8475.
13. Nigrey P. J., MacDiarmid A. G., Heeger A. J., *J. Chem. Soc. Chem. Commun.* **1979**, *14*, 594.
14. Winder C., Sariciftci N. S., *J. Mater. Chem.*, **2004**, *14*, 1077.
15. Kitamura C., Tanaka S., Yamashita Y., *Chem. Mater.*, **1996**, *8*, 570.
16. Jayakannan M., Hal P. A. V., Janssen R. A. J., *J. Pol. Sci. A Pol. Chem.*, **2002**, *40*, 251.
17. Chen M., Perzon E., Andersson M. R., Marcinkevicius S., Jönsson S. K. M., Fahlman M., Berggren M., *Appl. Phys. Lett.*, **2004**, *84*, 3570.
18. Ajayaghosh A., *Chem. Soc. Rev.*, **2003**, *32*, 181.
19. Tourillon G., Garnier F., Garzard M., Dubois J. C., *J. Electroanal. Chem.*, **1983**, *148*, 299.
20. Perepichka I. F., Perepichka D. F., Meng H., Wudl F., *Adv. Mater.*, **2005**, *17*, 1.
21. Ihn K., Moulton J., Smith P., *J. Polym. Sci. Part B Polym. Phys.*, **1993**, *31*, 735.
22. Brown G. H., *Photochromism*, **1971**.
23. Somani P. R., Radhakrishnan S., *Mat .Chem. Phys.*, **2002**, *77*, 117.
24. Deb S. K., Chopoorian J. A., *J. Appl. Phys.*, **1968**, *37*, 4818.
25. Chang I. F., Gilbert B. L., Sun T .I., *J. Electrochem. Soc.*, **1975**, *122*, 955.
26. Otero T. F., Cortes M. T., *Adv. Mater.*, **2003**, *15*, 279.
27. Cordova F. G., Valero L., Ismail Y. A., Otero T. F., *J. Mater. Chem.*, **2011**, *21*, 17265.
28. Demirci S., Emre F. B., Ekiz F., Oğuzkaya F., Timur S., Tanyeli C., Toppare L., *Analyst*, **2012**, *137*, 4254.
29. Paoli M. A. D., Gazotti W. A., *J. Braz. Chem. Soc.*, **2002**, *13*, 410.
30. Roncali J., *Chem. Rev.*, **1992**, *92*, 711.
31. Rathnayake H. P., Cirpan A., Delen Z., Lahti P. M., Karasz F. E., *Adv. Funct. Mater.*, **2007**, *17*, 115.

32. US Patent 5994836 “Organic light emitting diode (OLED) structure and method of making same” issued November 30, **1999**.
33. US Patent 4963196 “Organic solar cell” issued October 16, **1990**.
34. Heeger A. J., Nisbet T. R., *Solar Energy*, **1959**, *3*, 12.
35. Fang P.H., *Journal of Applied Physics*, **1974**, *45*, 4672.
36. Myers R. E., *Journal of Electronic Materials*, **1986**, *15*, 61.
37. Molander G. A., Bernardi C. R., *J. Org. Chem.*, **2002**, *67*, 8424.
38. Valle L. D., Stille J. K., Hegedus L. S., *J. Org. Chem*., **1990**, *55*, 3019.
39. Yamamoto T., Morita A., Miyazaki Y., Maruyama T., Wakayama H., Zhou Z. H., Nakamura Y., Kanbara T., Sasaki S., Kubota K., *Macromolecules*, **1992,** *25,* 1214.
40. Asavapiriyonont S., Chandler G. K., Gunawardena G. A., Pletcher D., *J. Electroanal. Chem.*, **1984**, *177*, 229.
41. Zaifoglu B., Sendur M., Unlu N. A., Toppare L., *Electrochim. Acta.,* **2012**, *85,* 78.
42. Neto B. A. D., Lopes A. S., Ebeling G., Goncalves R. S., Costa V. E. U., Quina F. H., Dupont J., *Tetrahedron,* **2005**, *61*, 10975.
43. Tsubata Y., Suzuki T., Miyashi T., Yamashita Y., *J. Org. Chem*., **1992**, *57*, 6749.
44. Zhu S. S., Swager T. M., *J. Am. Chem. Soc.,* **1997**, *119*, 12568.
45. Hanif M., Lu P., Li M., Zheng Y., Xie Z., Ma Y., Li D., Li J., *Polym Int.,* **2007**, *56*, 1507.
46. Zhang Y., Lai S. L., Tong Q. X., Chan M. Y., Ng T. W., Wen Z. C., Zhang G. Q., Lee S. T., Kwong H. L., Lee C. S., *J. Mater. Chem.,* **2011**, *21*, 8206.